Design and Development of Cost Effective Regenerative Braking System for Motor Operated Vehicle

A Thesis Submitted
in Partial Fulfillment of the Requirements for the Degree
of
MASTER OF SCIENCE IN
ELECTRICAL AND ELECTRONIC ENGINEERING

by

Adnan Mohammad

Supervisor

Dr. Md. Ziaur Rahman Khan

Professor, Department of EEE, BUET

Department of Electrical and Electronic Engineering

BANGLADESH UNIVERSITY OF ENGINEERING AND TECHNOLOGY

June 2017

APPROVAL

The thesis titled **"Design and Development of Cost Effective Regenerative Braking System for Motor Operated Vehicle"** submitted by **Adnan Mohammad**, Roll No: **0412062101 P**, Session: **April 2012** has been accepted as satisfactory in partial fulfillment of the requirement for the degree of Master of Science in Electrical and Electronic Engineering on 3rd June, 2017.

BOARD OF EXAMINERS

1. _____ Chairman (Supervisor)
Dr. Md. Ziaur Rahman Khan
Professor
Department of EEE,
Bangladesh University of Engineering and Technology (BUET)
Dhaka-1205, Bangladesh

2. _____ Member (Ex-officio)
Dr. Quazi Deen Mohd Khosru
Professor and Head of the Department
Department of EEE
Bangladesh University of Engineering and Technology (BUET)
Dhaka-1205, Bangladesh

3. _____ Member
Dr. Mohammad Jahangir Alam
Professor
Department of EEE
Bangladesh University of Engineering and Technology (BUET)
Dhaka-1205

4. _____ Member (External)
Dr. Md. Anwarul Abedin
Professor
Department of EEE
Dhaka University of Engineering & Technology (DUET)
Gazipur

Candidate's Declaration

It is hereby declared that this thesis or any part of it has not been submitted elsewhere for the award of any degree or diploma and the all sources are acknowledged.

Signature of the Candidate

Adnan Mohammad

To My Parents.

Acknowledgement

First of all, I would like to thank Allah for giving me the ability to complete this thesis work.

I would like to express my sincere gratitude to my supervisor, Dr. Mohammad Ziaur Rahman Khan for his coordination, patience and advices through the research. This thesis would not have been completed without his support and guidance. I would like to express my gratitude and gratefulness for his instructions, continuous encouragement, valuable discussions, and careful review during the period of this research. His perpetual motivation gave the confidence to carry out this work. I am thankful to him for providing all the necessary information and proper guidance.

I would also like to thank the authority of this university (BUET) for providing with the necessary assistance and allowing to use the university's laboratory.

My sincere gratitude to Dr. Md. Anwarul Abedin, Professor, Dhaka University of Engineering & Technology (DUET), for his precious time and fruitful suggestions.

I would also like to pay my solemn regards to my friends and colleagues who supported me generously and encouraged me enormously to complete this work.

Last but not the least, I would like to thank my parents. Their optimism and encouragement have allowed me to overcome any obstacle that I face. Their unconditional support made it possible for me to finish this thesis.

Abstract

Nowadays, the electric vehicles are becoming very popular due to easy operation, no fuel usage and smoother function. Moreover, the fare it takes from the passenger is quiet reasonable. However, it requires huge electric power to recharge the battery, which is the main source of energy for the vehicle. In addition, the existing braking system of the conventional transport is wasting some of the energies in the form of heat during the braking periods. Particularly, a rickshaw driver needs to brake the vehicle for several cycles. Hence, the wastage is a matter of concern.

Regenerative braking is a process of harnessing the stored kinetic energy in the form of electric energy during the brake period, where the motor of the vehicle operates as a generator and charges the battery. In this research, a new technique of the regenerative system is proposed and developed. It only uses the rectifier unit that naturally exists at the opposite side of the inverter, which controls the BLDC motor used inside the electric vehicle. Necessary units such as PWM circuit, microcontroller, gate driver circuits are implemented to achieve the proposed method of regenerative braking. To simulate the load performance a flywheel is designed and attached to the motor set. The back emf at different speed is recorded to select the proper charging system. After that, using the proposed method the battery is charged and successful outcome is seen. Furthermore, different characteristics such as, speed and back emf performances with varying duty cycles are noted. The response of the back emf with time is also observed and linearity is found. Based on the gathered data the energy regeneration is calculated for several speeds. Finally, a cost analysis is given at the end to justify the effectiveness. Overall, the proposed system can explore the commercial sectors of the recent electric vehicles and effectively store the braking energy in the form of battery charging. Additionally, the savings will be around 17.87 %.

Contents

List of Tables

List of Figures

List of Symbols

L	Inductance
C	Capacitance
R	Resistance
E_{an}	Back emf of phase ‘a’
E_{bn}	Back emf of phase ‘b’
E_{cn}	Back emf of phase ‘c’
E	Voltage Source
I_{bat}	Battery Current
Q1	Switching signal for switch ‘1’
Q2	Switching signal for switch ‘2’
Q3	Switching signal for switch ‘3’
Q4	Switching signal for switch ‘4’
Q5	Switching signal for switch ‘5’
Q6	Switching signal for switch ‘6’
H1	Pulse from the hall sensor ‘1'
H2	Pulse from the hall sensor ‘2'
H2	Pulse from the hall sensor ‘3'
PWM	Pulse Width Modulation

Chapter 1

Introduction

1.1 Introduction

Motor operated vehicle is becoming popular because it requires less physical effort and time to drive and it doesn't need any fuel like petrol, diesel or natural gas. As a result, research on electric vehicle becomes lucrative to enhance the flexibility and cost effectiveness of the overall system. Brushless DC (BLDC) motor used in many of these vehicles comes with different features such as, noiseless operation, better efficiency and electronic commutation [1]. As it eliminates the use of mechanical commutation, it becomes as a priority for the vehicle operators. However, The motor generally uses complicated control schemes, including fuzzy logic and field-programmable gate array control and the conventional mechanical braking system cause power loss in terms of heat as it has to work against the stored kinetic energy in the motor and affects the stability of the vehicle resulting frequent accidents during braking. Hence, the system becomes very sophisticated and expensive. The regenerative braking system, used in electric cars, is an energy recovery mechanism which slows down a motor by converting its kinetic energy into electrical energy while braking by charging the battery [2-3]. Conventional regenerative braking includes a boost converter and extra energy storing component (ultra-capacitor pack), which increase the cost and the size of the system [4]. In addition, multiple converters of the system cause extra power losses. This type of complicated system is not suitable for low cost electric vehicles that are becoming popular day by day. Hence, A flexible and cost effective control circuit with a regenerative braking system for the motors in electric vehicle is yet to be developed.

1.2 Significance of Motor Operated Vehicles

A motor operated vehicle operates using the battery system, which is the main source of power. Additionally, in the present time, most of the light electric vehicles use brushless dc motor for the necessary moving action [4-5]. In particular, these vehicles don't use fuel and petrol. Hence, electric Vehicles hold a lot of importance today. As they eschew the use of fossil fuel, the environment pollution is reduced and the cost of these systems is comparatively lower. Moreover, Electric vehicles have some lucrative features such as, a smoother operation, stronger acceleration and are quieter as compared to conventional vehicles with Internal Combustion Engine.

1.3 Conventional Braking System

There are various braking system in the electric vehicles. Some of the vehicles use the traditional braking system based on friction. In such systems, continuous braking is applied, which produces friction and stops the wheels from rotating, thereby slowing down the vehicle. This mechanism uses continuous brake that stops the rotations and friction is produced [6]. In addition, this friction generates heat and energy is wasted in the form of heat. The second brake system is the Anti-Lock brake system that uses a non-continuous braking pattern to slow or stop the vehicle as required. The latter system is more efficient than the conventional braking system and gives a superior performance. Another type of braking system is the regenerative braking system. In such a system, the motor itself or any other circuit works to apply the brakes by controlling the current in the motor circuit. Such types of systems also recharge the battery and help in braking. However, such brake systems cannot be used solely as they can slow down the vehicle, but generally do not bring it to a complete stop. Hence, such systems are used in conjunction with conventional friction brakes braking System. Additionally, they use the boost converter that increases the magnitude of back emf and charges the battery.

1.4 Regeneration Mechanism

Generally, the motor in the electric vehicle is run by a battery. During the braking, the kinetic energy of the motor is converted into heat energy due to friction and is subsequently lost. Regenerative Braking is an energy recovery system which tries to recover this energy before it is converted into heat [2-3]. This temporary energy can be harnessed following some voltage boost procedures and sending it back to the battery. Additionally, the motor acts a generator during the regenerative braking period. Shortly, the battery receives energy from the motor. Alternatively, the current going to the electric motor while braking can be diverted and stored. This method uses different circuitry such as, boost converter, super-capacitor methods etc.

1.5 Characteristics of the Electric Vehicles

The current electric vehicle system has several merits such as, it has no emission and does not pollute the environment, the operation is quiet if compared with others, precipitated acceleration system, no fuel consumption and cost effective, higher efficiency and no dependency on fossil fuel like diesel or petrol [7].

However, there are some drawbacks in electric vehicles. The range of the electric vehicle is around 150 to 200 kilometers, while the gasoline vehicles have a larger range of up to 300 kilometers. It takes long time for charging purposes and the battery pack are large and requires more space.

1.6 Earlier Research on Regenerative Braking

Electric vehicles have electric motors inside their structure and regenerative braking can be incorporated. In the regenerative braking operation the motor operates as a generator. The regenerative braking systems are applied in two and three wheeler vehicles [8].However, this scheme includes many of the additional hardwares [9]. The battery pack has significant role for getting distance and it should be used carefully. Therefore, it uses extra units for careful and efficient operations. In this regard, the super capacitor technology is used for effective energy

usage and it also extends the lifetime of the battery [10]. Generally, the supercapacitor is connected in shunt with the battery bank. Recently, many analyses about regenerative braking are performed by different perspectives. One of the most common practices is to usea boost converter system to harness the braking energy.

In the boost converter based scheme, the back emf is increased and then the battery is charged. In particular, the back emf of a motor is always less than the battery voltage. Hence, it is obvious to boost the magnitude of the back emf to transfer the energy into the battery. To accomplish the charging operation, the boost converter is connected with the motor terminal and the higher voltage is obtained controlling the duty cycle of the switching pulses.

An ultracapacitor bank regenerative braking control system for an electric vehicle has been analyzed [11-13]. The system allows higher accelerations and decelerations of the vehicle with minimal loss of energy. In this method an IGBT Buck-Boost converter is used, which is connected to the ultracapacitor bank at the Boost side, and to the main battery at the Buck side. The control system measures the battery voltage, the battery state-of-charge, the car speed, the instantaneous currents in both the terminals (load and ultracapacitor), and the actual voltage of the ultracapacitor. Thelevel of actual voltage allows to know the amount of energy stored in the ultracapacitor. A microcontroller control is used to generate the PWM switching pattern of the IGBTs. When the vehicle is accelerating, the battery voltage goes down, which is an indication for the control to take energy from the ultracapacitor. In the opposite situation where regenerative braking is concerned, the battery voltage goes up, and then the control needs to activate the Buck converter to store the kinetic energy of the vehicle inside the ultracapacitor. The measurement of the currents at both sides allows to keep the current levels inside maximum ratings. The battery state-of charge is used to change the voltage level of the ultracapacitor at particular values. If the battery is fully charged, the voltage level of the capacitors is kept at lower level that is below the partially discharged battery. The converter also has an IGBT controlled power resistor, which allows to drop energy in some extreme situations that cannot be accepted neither for the ultracapacitors nor for the battery pack.

The regenerative braking energy recovery control strategies for electric vehicle (EV) based on fuzzy logic control and FPGA control are proposed [14-16]. The sugeno fuzzy logic controller (FLC) is developed by analyzing the characteristic of the regenerative braking.Simulation experiments with different driving cycles were carried out, and the feasibility and effectiveness of the fuzzy logic control strategy are tested with the state of charge (SOC) and braking energy recovery.

However, these methods require auxiliary components that not only increase the cost of the overall system but also the size as well. Hence, there is a scope for further research to reduce the cost involved and space requirements.

1.7 Objectives

The objectives of this thesis are to:

i. Design and implement a three phase inverter for operating a BLDC motor used for motor operated vehicles and generate the required switching pulses for controlling the motor operation via Microcontroller.

ii. Design a simpler and cost effective regenerative braking system,

iii. Analyze the proportion and variation of energy regeneration during braking withdifferent motor parameters and operating conditions (under loaded condition), and thestability of the system.

The successful implementation of this work can explore the possibility of regenerative braking for the battery driven motor operated vehicle and thus enhance the energy efficiency and stability of the vehicle system.

1.8 Thesis Organization

This thesis is divided into chapters for presenting a structured view of the developed work. Inthis introductory chapter the main purposes and motivations of the work are presented with the current state of the problem.

Since this thesis develops a regenerative braking system of low cost electric vehicle, Chapter 2 represents the major components of the implementation. In Chapter 2, we start with the general explanation of different components used to develop the three phase inverter and control system. The features and operations of several components are presented.

Chapter 3 describes the simulation parts of the three phase inverter and shows the simulated outputs of the control system. All parts are depicted step by step and simulated according to the desired switching. It also illustrates the simulation of the microcontroller system.

In Chapter 4 the details of the hardware implementation are presented following the former chapter. The Outputs of PWM circuit, microcontroller, gate driver and inverter are carefully noted. After that, the BLDC motor is connected with the outputs of inverter. A flywheel is designed to justify the loaded operation. Speeds at different duty cycle are noted and corresponding back emfs are monitored. Finally, the proposed regenerative braking system is experimentally verified.

Conclusion over the entire work that has been done is made in Chapter 5. This chapter also suggests the possible future opportunities and scopes of this study.

Chapter 2

Motor Operated Vehicle and Regenerative Braking System

2.1 Introduction

In this chapter detail discussion on different types of motor operated vehicles and regenerative braking system will be done. Firstly, operation and construction of electric vehicle will be explained with their features. Next, various braking systems and recent research on regenerative braking will be illustrated with their limitations. Finally, their corresponding outputs will be widely shown to scrutinize the overall system.

2.2 The Structure of Electric Vehicles

In this portion, the construction of different electric vehicle such as, three wheeler and electric rickshaw will be described. It will also show the motor set up inside the vehicle.

2.2.1 Construction of the Electric Rickshaw

In the recent time there is no doubt that battery operated vehicle is robust and strong enough. Also, it is ensured that this vehicle provides all the facility for the comfort of every passenger. Additionally, there are lots of E-Rickshaw spare parts required for the construction of E-rickshaw. Also, the vehicle is crafted with the best quality of metal and fiberglass. Among the other materials, an open frame is used for the construction of these E-rickshaws. The rickshaw is no doubt cost-effective because it is battery operated as well as consumes less energy.

Figure 2.1 : The three wheeler E-rickshaw [17-18]

The general three wheeler found in the present market is shown in the Figure 2.1. The 3 wheeler E- rickshaw is definitely the best substitute for fuel driven vehicles and efficient when comes to battery power. Also, there is no emission of harmful pollutants from this vehicle so it helps to increase the durability and strengthens the vehicle. The materials which are used in constructing the vehicle such as fibreglass help it to make the vehicle more efficient. Also, this vehicle is absolutely perfect to cover the short distance as well as carry small loads.

These rickshaws have a mild steel tubular Chassis, consist of 3 wheels with a differential mechanism at rear wheels [18]. The motor is brushless DC motor manufactured mostly in India and China. The electrical system used in Indian version is 48V and Bangladesh is 60V. The body design from most popular Chinese version is of very thin iron or aluminum sheets. Vehicles made in fiber are also popular because of their strength and durability, resulting in low maintenance, especially in India. The Body design is varied from load carriers, passenger vehicles with no roof, to full body with windshield for drivers comfort. It consist of a controller unit.They are sold on the basis of voltage supplied and current output, also the number of MOSFET used. The battery used is mostly lead acid battery with life of 6–12 months. Deep discharge batteries designed for electric vehicles are rarely used. Weight of the electric car has also been a recurring design difficulty in them.

2.2.2 The Motor Set Up

Figure 2.2 : BLDC motor inside the rickshaw

The general motor set up is given in the Figure 2.2. It is put on a structure designed for motor position beneath the rickshaw seat. The two back wheels are attached with the chain, which rotates with the motor. The gear is given to adjust the speed of the vehicle. The front wheel of the rickshaw is not directly with the motor.

2.2.3 The Controller Unit

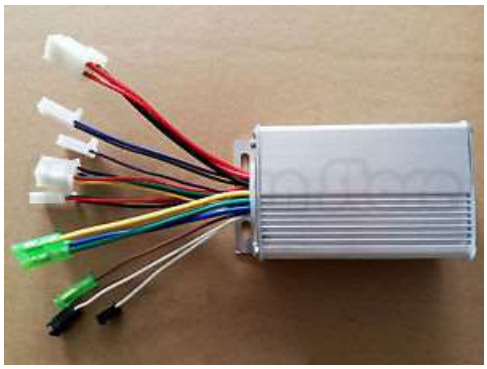

Figure 2.3 : The controller

In the Figure 2.3 the controller unit is shown. It is basically a three phase inverter with necessary signal conditioning units. Different wirings are available for proper operation and connections. This unit is also directly connected with the battery. Additionally, the output of the controller goes to the motor.

2.3 Recent Analysis on Regenerative Braking Systems

In this section, several current methodologies of regenerative braking system will be explained. Various methods such as, boost converter based braking and ultra-capacitor based braking system will be discussed. Then, some of the algorithms based on which the motor control systems operate will be recalled to provide a wider area of research.

2.3.1 Boost Converter Based Regenerative Braking of BLDC Motors

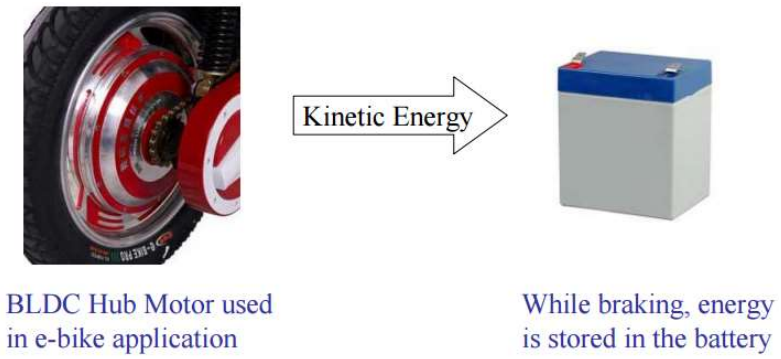

Figure 2.4: Regenerative braking in E-bike application

The concept of regenerative braking is shown in Figure 2.4 [19]. Regenerative braking stores energy back into the battery, while increasing the life of friction pads on brake shoe. However, to bring the bike to a complete stop, the mechanical brakes are required.

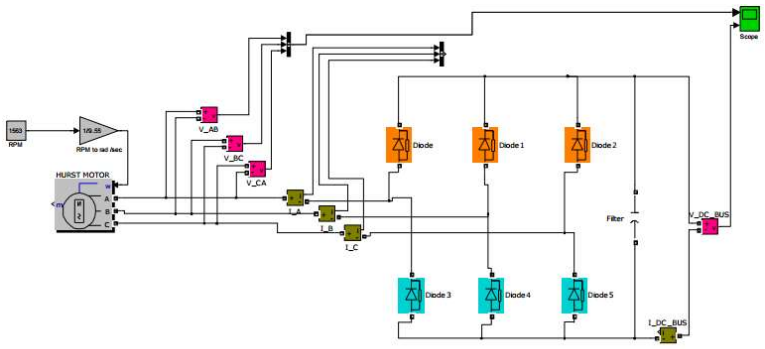

Figure 2.5: The operation of back emf rectifier

The Figure 2.5 shows the rectifier unit that rectifies the sinusoidal back emf of the BLDC motor operating as the rotating parts of an electric vehicle. In particular, this analysis is performed for the Hurst BLDC motor. The Hurst BLDC motor running at 1563 rpm, generates the EMF, which is rectified by a 3 phase diode configuration and filtered to DC to charge the battery.

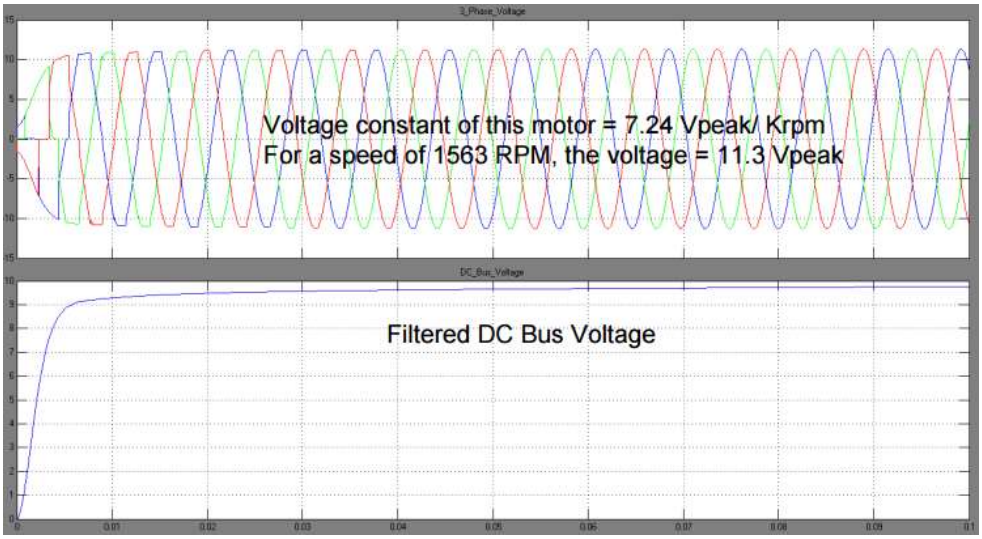

Figure 2.6: Three phase rectifier simulation results

The simulation of the three phase rectifier is given in the Figure 2.6. It also shows the filtered dc voltage that will be boosted to recharge the battery. The dc voltage is around 10 V.

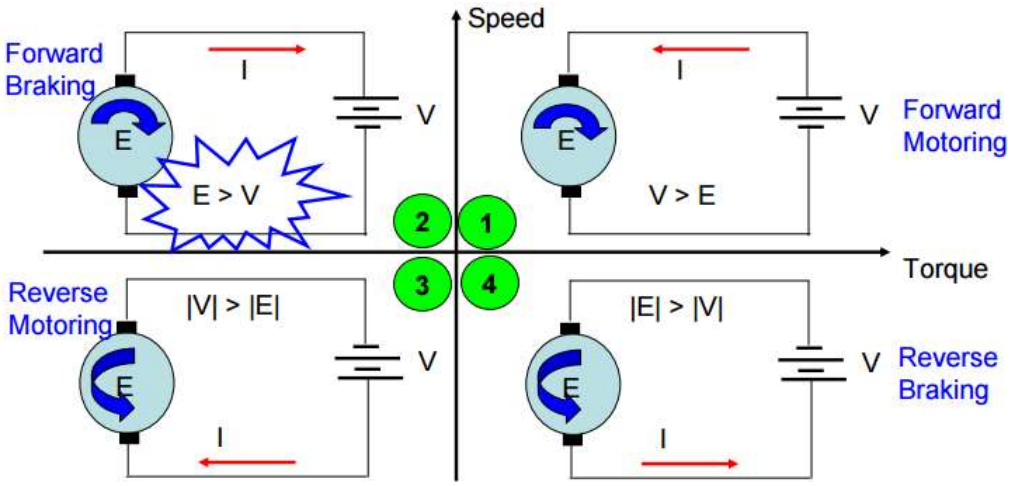

Figure 2.7: 4-Quadrant motor operation

For a BLDC motor to operate in 2nd quadrant, the value of the back EMF generated by the BLDC motor should be greater than the battery voltage (DC bus voltage). This ensures that the direction of the current reverses, while the motor still runs in the forward direction. This above explanation is delineated in the Figure 2.7.

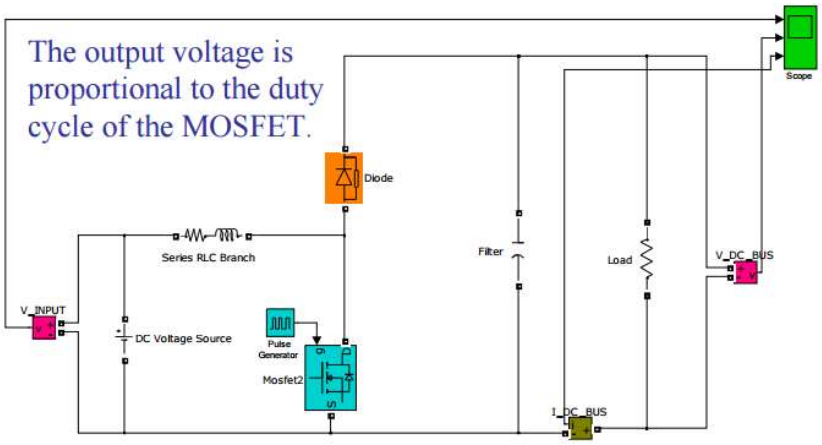

Figure 2.8: Boost converter

The boost converter is used to increase the magnitude of rectified back emf. The Figure 2.8 shows the simulation circuit of the boost converter. The magnitude of the output voltage of the boost converter is dependent on the duty cycle.

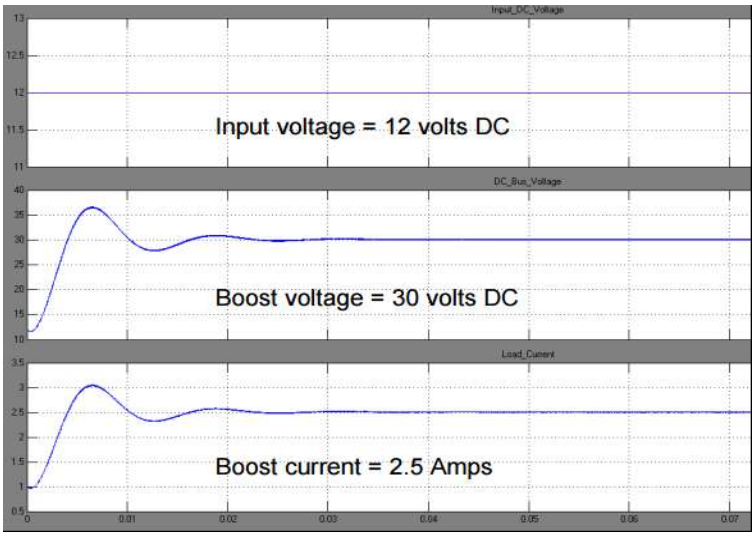

Figure 2.9: Boost converter simulation results

The simulated output is shown in the Figure 2.9. The output voltage is around 30 V and current is 2.5 A. Hence, a successful boost operation is achieved. The voltage level depends on the on time of the switches or duty cycle.

2.3.2 Ultra-Capacitor Based Electric BicycleRegenerative Braking System

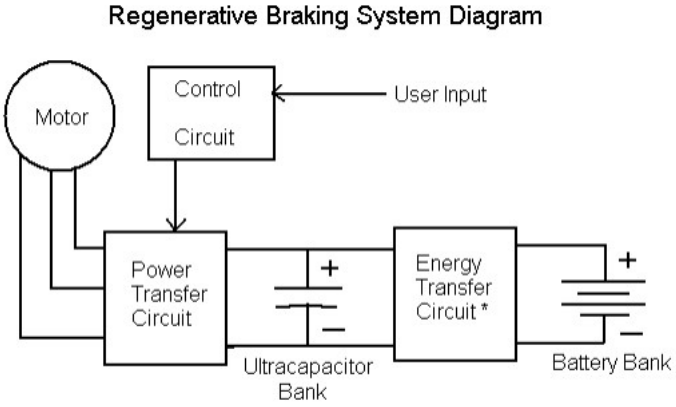

Figure 2.10: The regenerative braking system with ultra-capacitor [12]

A regenerative braking system, including the ultra-capacitor is proposed in the Figure 2.10. Ultra-capacitor based regenerative braking applications are currently, for the most part, restricted to hybrid buses and railway cars, where stops are predictable, and space is not too much of an issue. For this experiment these applications were outside of the author's budget, so a smaller scale electric bicycle was used instead, in order to measure ultra-capacitors' ability to recoup braking energy. A 650 Farad Boostcap manufactured by Maxwell Technologies can be purchased by an individual consumer for roughly $60 through distributors such as Tecate Group [ultra]. The 650 F capacitor used in this project is rated for 60 A of continuous current. Charging a similar sized lithium battery at 20 A would not be recommended. The 650 F capacitor is about the size of a tangerine. Ultra-capacitors can also withstand hundreds of thousands of charge cycles without losing their ability to store charge, thus making them more suitable for high stress applications such as regenerative braking. Special considerations need to be taken when using these devices, however. As opposed to batteries, ultra-capacitors behave just like regular capacitors, in that the energy stored in their electric field follows the $E_C = ½CV^2$ law, where E_C, the energy stored, is in Joules, the capacitance C is in Farads and V in Volts. A 650 F Ultra-capacitor Source: Alex Bronstein 4 Moreover, a capacitor with less charge on it is easier to charge, because smaller voltages are needed to transfer charge onto its plates. Therefore for the most energy to be absorbed it is best for the capacitors to have as low of charge state as possible when braking is engaged.

2.3.3 Buck-Boost Converter Based Regenerative Braking System

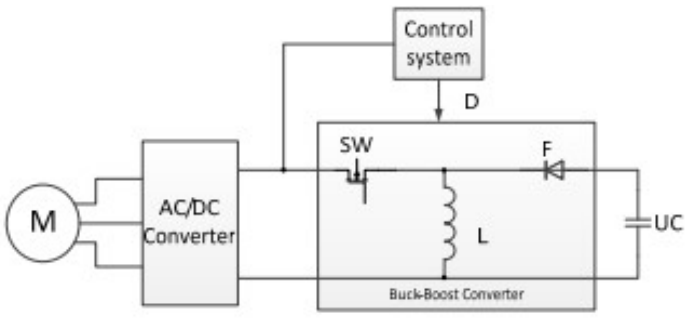

Figure 2.11: The regenerative braking system with buck-boost converter [20]

Another process of regenerative braking that is shown in the Figure 2.12 uses a buck-boost converter with the ultra-capacitor [20]. The process of regenerative braking of an electric vehicle with a source of energy - battery and ultra-capacitor is subject of this work. The studied system is composed of a brushless DC motor, buck-boost DC converter and ultra-capacitors. An optimization of the control system for storing maximum energy in the ultra-capacitors is performed. The results are useful for the aim of improving the control of energy flows in electric vehicle and achieving a maximum range with a single charge.

Regenerative braking is an efficient way for improving electric vehicles dynamics and extension of the battery life. As a result from the mentioned research, the following conclusions are given such as, the amount of energy stored in the ultra-capacitors depends slightly on the switching frequency of the DC converter, losses in the converter are proportional to the switching frequency, the ripple of the motor current is practically independent from the filter inductance L, and the control system is invariant from the amount of energy recovered and the converter parameters. The influence of the regulator settings on overall system efficiency is weak. The majority of losses in the system is in the ultra-capacitors. A natural extension of this research is a study of the outer control loop of the system.

2.4 Conclusion

This chapter contains the detail discussion of the electric vehicle system. In particular, it describes the structure of different battery driven transports. Then, it shows the motor and its set up including the controller unit. After that, various regenerative braking procedures are discussed and recent research on the braking system is illustrated.

Chapter 3

Experimental Setup of the Proposed System

3.1 Introduction

In this chapter, the proposed system will be discussed. After that part, the operation of brushless DC motor and inverter switching are studied and then a pulse width modulation circuit and a circuit containing hall sensors are designed to provide input into the microcontroller, which is coded to perform the desired switching for the three phase inverter. Then, necessary printed circuit board layouts are designed and printed for the circuits such as gate driver, pulse width modulation circuit, comparator and three phase inverter which are implemented in hardware for practical data analysis.

A flywheel weighted approximately 10 Kg is attached to the motor to store its kinetic energy, so that significant regenerative braking can take place. In this process, the motor is run at different speeds by varying the duty cycle of PWM circuit using a potentiometer.

3.2 The Proposed Regenerative Braking System

Figure 3.1 illustrates the flow chart of the electric vehicle control system. The controller (microcontroller) of Figure3.2 determines the motor operation. The microcontroller generates the desired pulses to operate the BLDC machine sensing the PWM and signal from hall sensor. Arduino microcontroller is used in this research.

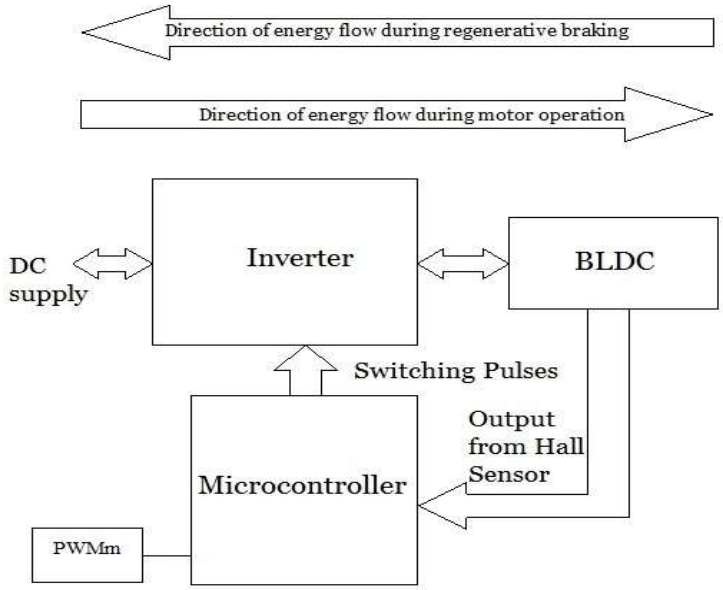

Figure 3.1:Flow chart of electric vehicle control system

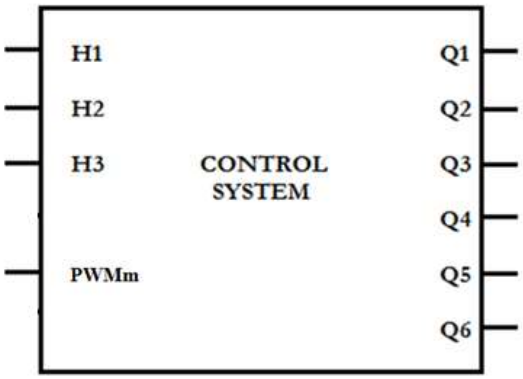

Figure 3.2:The controller

The circuits for the proposed system are depicted in the Figure 3.3 amd3.4. During motor operation, the switch 'S' will at P1. Hence, the inverter will drive the motor and power will flow from the batteries to the motor following the particular switching. However, during the braking time, 'S' will be at P2 and the power will now flow from the motor side to the battery side charging the bottom battery. It is important to note that, for MOSFET protection, a diode in reverse parallel connection is provided with every MOSFET. Such types of protection prevent the damage of MOSFET during inductive load operation. Hence, a three phase inverter can act as a three phase rectifier in reverse direction.

The rectified back emf at the rated speed (450 rpm) is around 33 V. As a result, at different speed 2 batteries out of 4 can be charged. When the back emf is above 24 V, two batteries can be charged, while only the lower side battery can be charged for a back emf below 24 V and above 12 V (Figure 3.3).

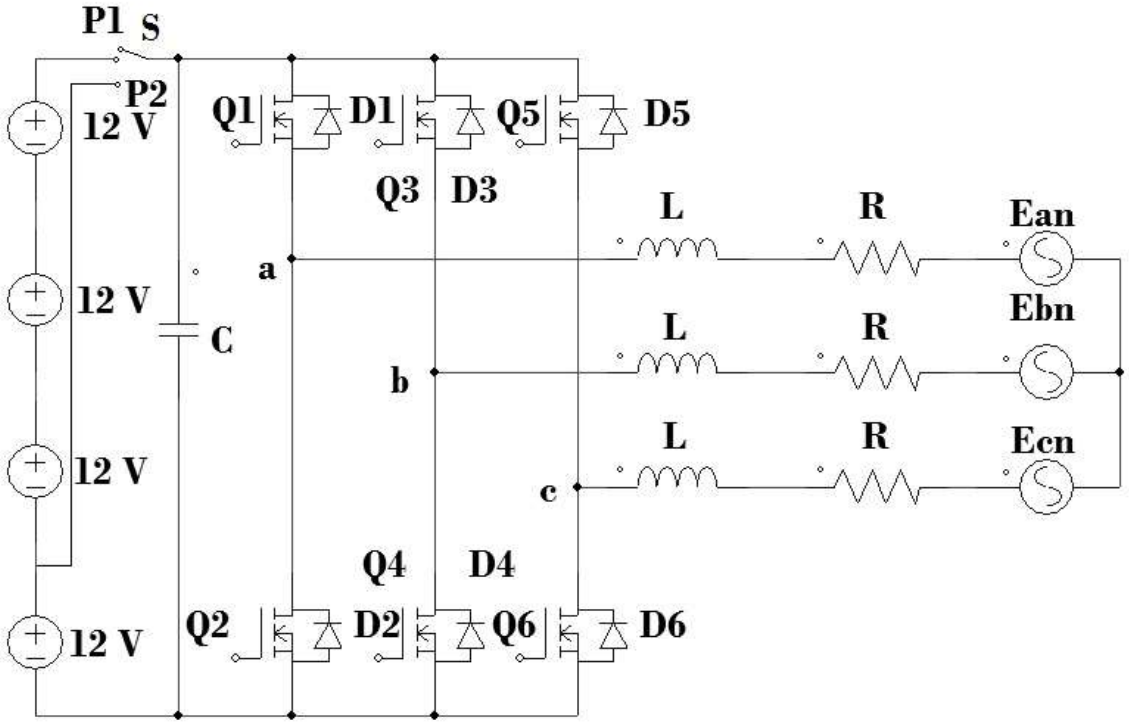

Figure 3.3 : The circuit diagram for proposed braking system (12 V System)

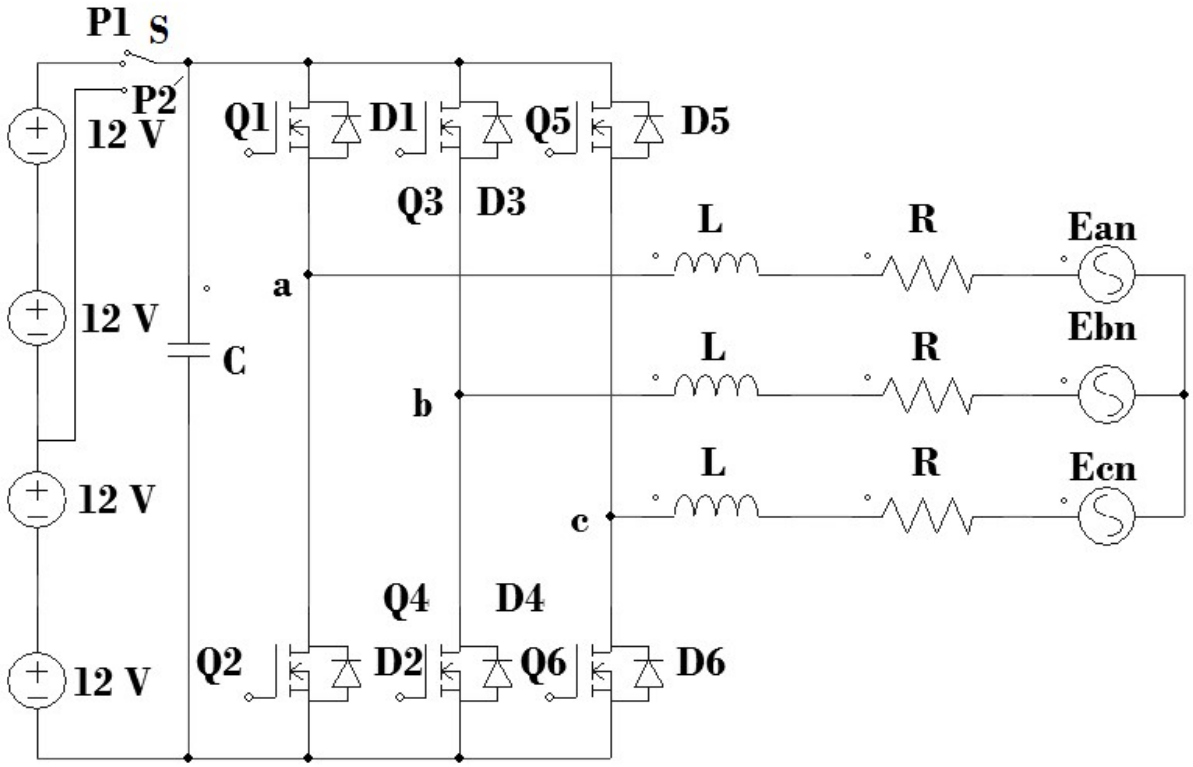

'S' at P1 : Power flows from the battery side to motor through the inverter.

'S' at P2 : Power flows from the motor`s back emf to the indicated battery by the rectifier that exists at the opposite direction of the inverter.

Figure 3.4: The circuit diagram for proposed braking system (24 V System)

The proposed system for the 24 V charging system is shown in the Figure 3.4. Here, during motor operation 'S' will be at position P1 and braking will take place at P2/.

3.3 Operation of the Circuits

This section deals with the operations of different circuits such as three phase inverter, brushless dc motor, pwm circuits, microcontroller and etc. Furthermore, simulations are given to provide glimpse of the practical results.

3.3.1 Description of Inverter and Motor Operation

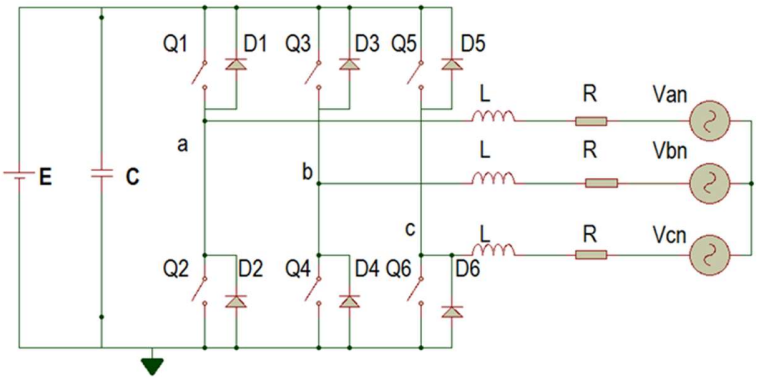

Figure 3.5: Inverter circuit and BLDC motor

Figure 3.5 shows the electric vehicle control system which uses three phase inverter and BLDC motor . In this circuit E is the input DC voltage, C is the filter capacitance, Q1 to Q6 switches which form the inverter circuit, D1 to D6 are freewheeling diodes used to protect the switches, L is the motor winding inductance and R is the motor winding resistance. The back emf(s) of the motor are represented by Van, Vbn and Vcn.

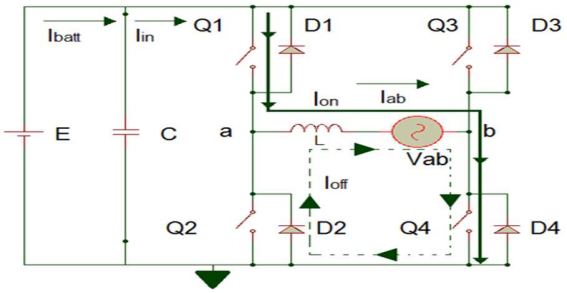

Figure 3.6: Equivalent circuit of BLDC machine for motoring action

To explain the operation of BLDC motor one complete cycle of 360 ° can be divided into six intervals [21-22]. Figure 3.4 shows the equivalent circuit for 60° interval. This interval of operation is divided into two states for motor operation. Switch

Q1 and Q4 remain ON in the first state of operation in which current flows from E to motor (‘a’ to ‘b’). In the next state of the operation switch Q4 remains ON (Q1 OFF) and the stored energy in the motor inductor during the first state of operation releases via Q4 and D2.

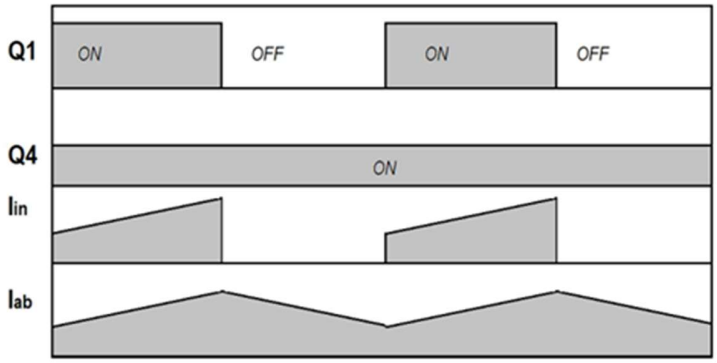

Figure 3.7:Switching states and current waveforms for motoring mode

Figure3.7depicts the waveforms and switching state for motor operation. In this Figure, Iin is the input current which flows from the supply to the motor and Iab is the motor terminal current. In motor mode of operation switch Q4 remains ON for both of the states.

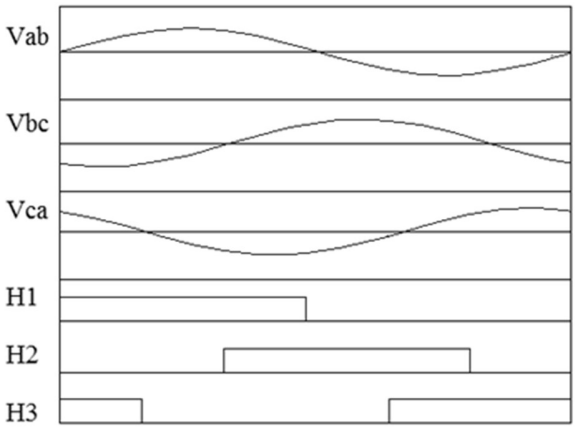

Figure 3.8:Back emf and Hall sensor pulse

Figure 3.8 shows the back emf waveforms of BLDC motor and outputs of hall sensors. The phase difference of back emf is 120°. Three hall sensors are used to detect the rotor position of BLDC motor [23-25]. H1 to H3 are the outputs of hall sensor. The outputs have 120° phase difference and 50% pulse width. BLDC motor control algorithms are based on these pulses.

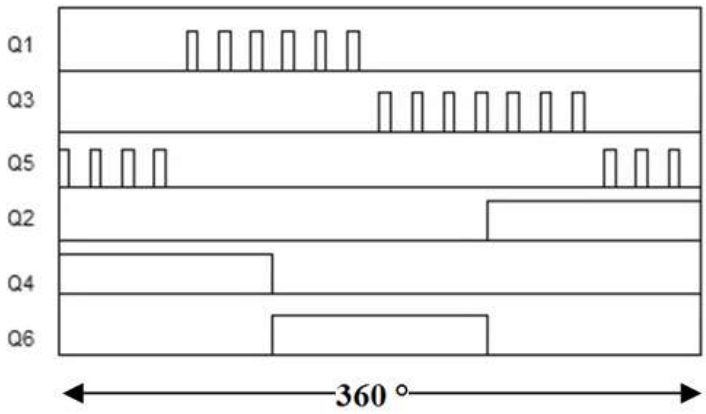

Figure 3.9:The motoring pulse

Figure 3.9 shows the necessary control signals for motor and regenerative braking operation in one full cycle. Operation for one interval (out of six) has been discussed.

3.3.2 Operation of the Microcontroller

In this section, control pulses generated by a microcontroller will be shown. These pulses will operate the inverter which drives the BLDC machine in motor mode. It is necessary to write code for microcontroller based on the control algorithm. The control algorithm for the desired operation is provided based on Figure 3.9.

$$Q1 = H1.\overline{H3}.(PWMm) \tag{3.1}$$

$$Q3 = \overline{H1}.H2.(PWMm) \tag{3.2}$$

$$Q5 = \overline{H2}\ H3\ (PWMm) \tag{3.3}$$

$$Q2 = \overline{H1}.H3 \tag{3.4}$$

$$Q4 = H1.\overline{H2} \tag{3.5}$$

$$Q6=H2\overline{H3} \tag{3.6}$$

Equation (3.1) to (3.6), present the control logic for the motor. Here, Q1 to Q6 are the pulses for six switches. H1 to H3 are the hall sensor output, PWMm is the pulse of motor operation.

3.3.3 PWM Circuit

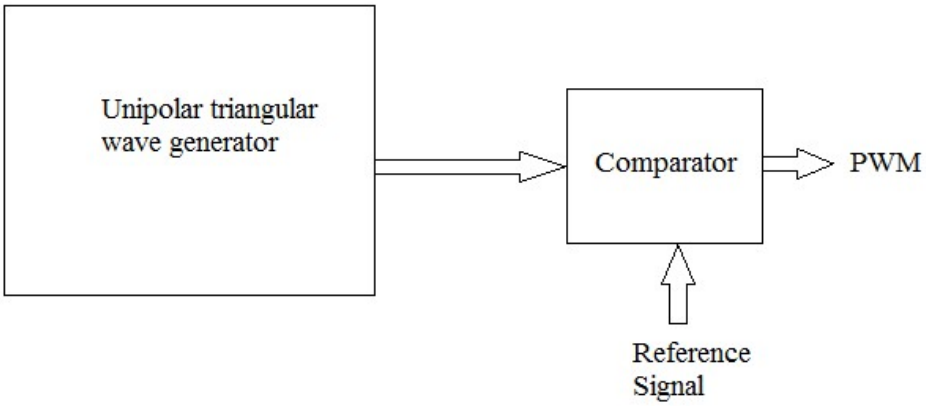

Figure 3.10: PWM signal generating block

This unitis designed to obtain switching signals of varying widths. A unipolar triangular wave is generated and compared with a variable reference signal to get different duty cycles.

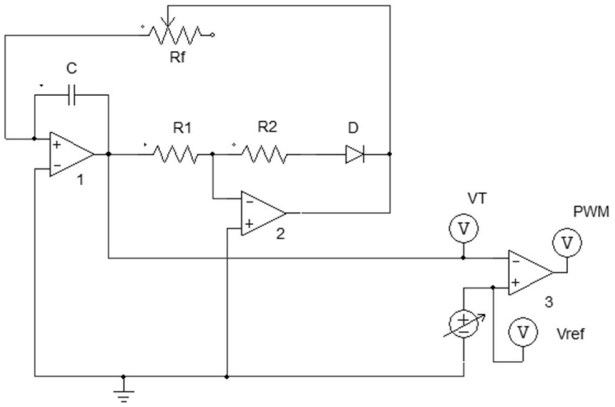

Figure 3.11: PWM generation circuit

The pwm generation circuit is given in Figure 3.11. Three operational amplifiers are used to accomplish the PWM technique. First two operational amplifiers are used to generate unipolar

triangular wave which is then given to pin 2 of the third op-amp. To get unipolar triangular wave the didode ‘D’ is used in the circuit. Furthermore, a reference voltage is applied to the pin 3 to adjust the duty cycle of the pwm signals. This variable voltage can be generated using the voltage used for biasing pin 7 of op-amp and a variable resistance. The frequency of the system can be changed using the variable resistor ‘Rf’. The necessary equations including that of frequency are given below [26],

$$Vp = \frac{-Vsat + 0.6V}{p} \tag{3.7}$$

$$f = \frac{p}{2RC} \tag{3.8}$$

$$\mathrm{R2} = \mathrm{p}.\,\mathrm{R1} \tag{3.9}$$

In these equations, Vp is the peak of the triangular waveform, Vsat is the bias voltage, f is the triangular wave frequency which is dependent on a resistance ‘R’ and capacitance ‘C’of the circuit and a multiplying factor ‘p’ which can be set at 1.

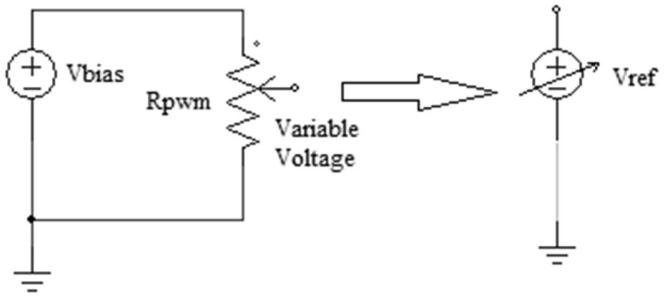

Figure 3.12: Generating variable reference voltage

Figure 3.12 shows the technique to generate variable reference voltage which is used to vary the pulse width of the switching signals. A potentiometer is connected to the bias voltage used to operate op-amp, and the variable voltage is obtained between the ground and variable pins of the potentiometer. This is easily done as the input impedance of op-amp is infinity and cannot introduce loading effect on the variable voltage across the potentiometer.

3.3.4 Hall Sensors and Comparators

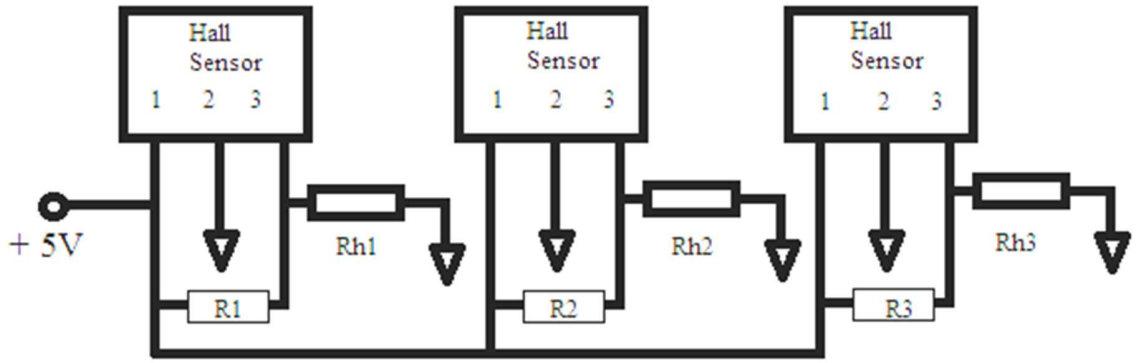

Figure 3.13: Hall signal generation

Figure 3.13 shows the hall sensor signal generation circuit. Three Hall sensors in form of IC are used inside the motor and they have three pins. Pin 1 of each is connected with a 5 V source for their biasing. Pin 2 is the ground pin and three resistors (Rh1, Rh2 and Rh3) are connected between the output pin 3 and ground to get pulses from hall circuit. It is important to mention that, they come inside the motor with a particular mechanical displacement of 120 degree.

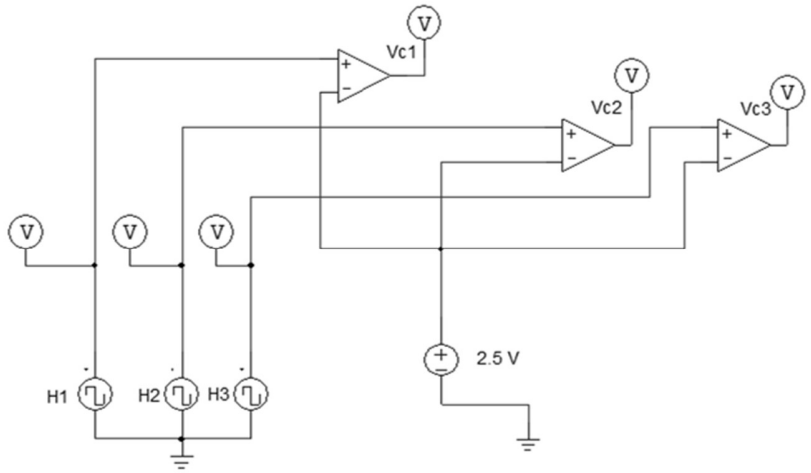

Figure 3.14: Three comparators

Direct connection of hall circuits with microcontroller disrupts the system and motor becomes OFF either by short circuit or open circuit condition which is due to the false operation of microcontroller system. Hence, three comparator circuits are designed to generate the similar output pattern of hall circuits` outputs by comparing these with a voltage smaller than the peak of hall outputs.

3.3.5 The Gate Driver Circuit

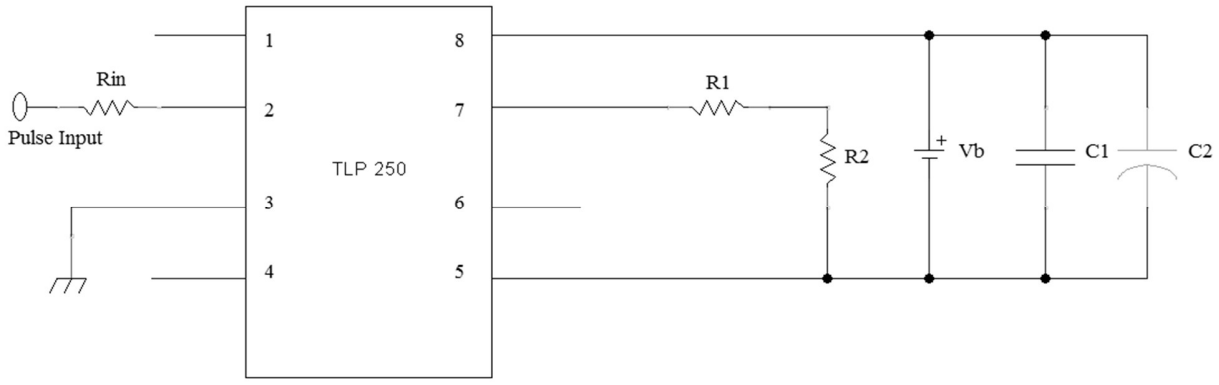

Figure 3.15: Gate driver circuit

Figure 3.15 shows the gate driver circuit which is designed to provide isolation between microcontroller and three phase inverter circuit. Particularly, it applies the gate pulses between the gate and source terminals of the MOSFET.

The IC used here is TLP 250 which has 8 pins. The input to the gate driver circuit from microcontroller is given between 2 and 3 pins. A resistor Rin connected to limit the input current. The output is taken across R2. This output follows similar input pattern. The biasing voltage 'Vb' is applied between pin 8 and 5. Capacitors are used to block ac components. It is important to note that, the output can be taken either from pin 6 or 7. In addition, unused pins are 1 and 4.

3.3.6 Block Diagram of The BLDC Motor System

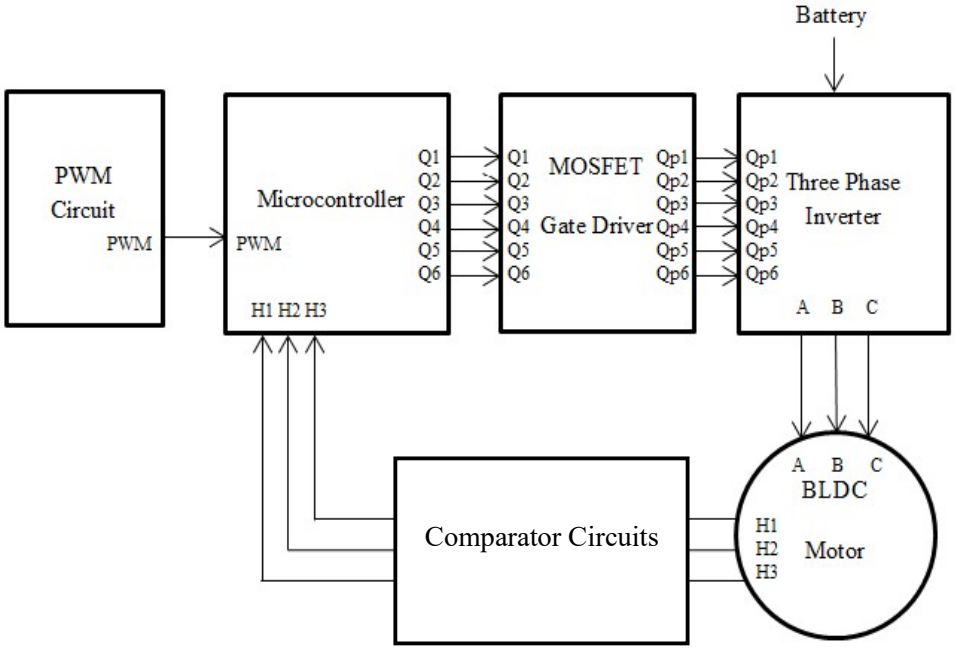

Figure 3.16: Block diagram of the hardware set up

The overall hardware set up is shown in Figure 3.16. A circuit is designed to perform PWM. The microcontroller is coded to generate the required switching based on the inputs PWM, H1, H2 and H3. The output of the microcontroller is given to the gate driver circuit which is used to provide isolation between the control and main power circuit (inverter). A brushless dc motor is connected as load with the three phase inverter. The hall sensors are used to detect the rotor position, which is very important for applying perfect switching to the inverter. Three comparators, which generate outputs similar with that of hall sensors, are designed to discontinue the direct connection between sensors and microcontroller. Particularly, following this technique microcontroller`s false operation which collapses the system (either making short circuit or open) can be avoided. Variation in speed is achieved using different widths of switching pulse. Both line to line and phase voltages are observed.

3.3.7 SimulationCircuit of The Three Phase Inverter

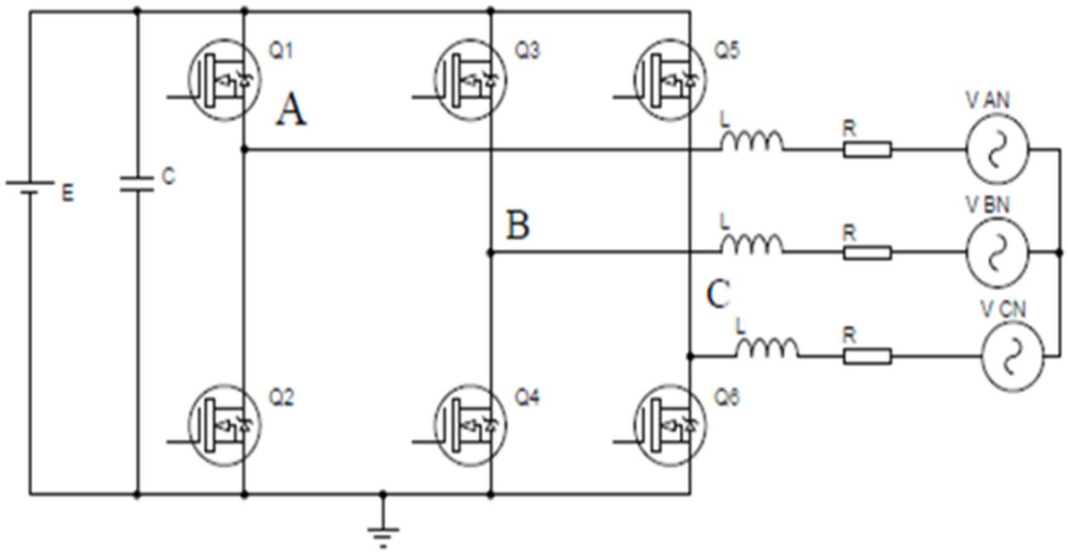

Figure 3.17: Simulation circuit for the three phase inverter

The Figure 3.17 shows the three phase inverter circuit for simulation purpose. In this case, the switches have been operated following the previous operating principle. Here, L and R represent the motor inductance and resistance respectively. VAN, VBN and VCN are back emf of BLDC motor. E is the battery and C is the input capacitor of the inverter. This inverter consists of six switches Q1 to Q6. The three phase output is taken from A, B and C. The generated back emf of the motor used in sinusoidal in nature. Hence, three sinusoidal sources are used to justify the behavior of the motor.

3.4 Description of the Components

In this portion, the features of the components which are used to construct the system, will be explained with their figures. In addition, the components used here are of different types such as; passive, electronic and electrical.

3.4.1 Diode

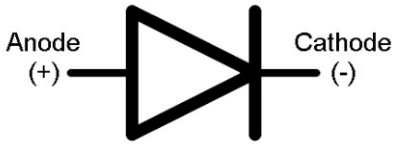

Figure 3.18: Diode

A diode is a two-terminal electronic component that conducts mainly in one direction; it offers zero resistance to the flow of current in one direction, and infinite resistance in the other. The name of the terminals are anode and cathode. The potential of anode terminal must be greater than the potential of the cathode for operating a diode.The most common type semiconductor diode today, is a crystalline piece of semiconductor material with a p–n junction connected to two electrical terminals [27]. A void tube diode has two electrodes, a plate and a heated cathode. Semiconductor diodes were the first semiconductor electronic devices. Today, maximum diodes are made of silicon, but other semiconductors such as selenium or germanium are moderately used.

3.4.2 Operational Amplifier

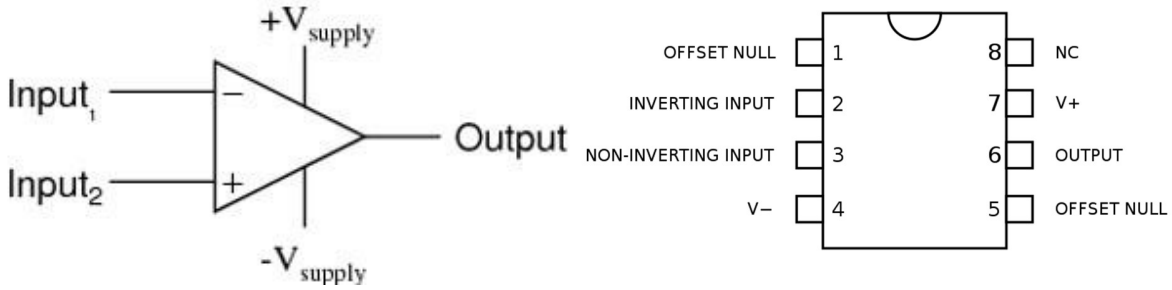

Figure 3.19: Symbol and block diagram of operational amplifier

Figure 3.19 shows the symbol and block diagram of an operational amplifier which is one of the most versatile and extensively used IC is operational amplifier. It is called an operational amplifier as it can perform mathematical operations. Initially it was used to add, subtract.

Multiply and differentiate [26]. However, it can be used to generate triangular wave which can be used as input to perform PWM for the switching the power electronic converters and as a comparator. It is also well known as IC741. It has eight pins which consist of two biasing pins, two input pins (inverting and non-inverting input pin), one output pins and so on. The most important feature is its higher input impedance which can nullify the loading effect of a system. Moreover, it has more features such as; Short circuit and overload protection, low power consumption, large common mode rejection ratio (CMRR) and differential voltage ranges, no requirement of external frequency compensation and no latch-up problem. It also does not need any external compensation for phase component. This simplifies the circuit design and minimizes the number of components used. One important issue that should be known during its use is that, the dc output voltage will be zero if both the inputs of the 741 IC are connected to the ground. But in practice, a small dc output may appear due to minor internal unbalances. It is usually unnoticed in normal applications. But for critical conditions, the output voltage can be set precisely to zero by connecting a 10K potentiometer between terminals marked “offset-null”.

3.4.3 Microcontroller (Arduino Uno)

Figure 3.20: The Arduino Uno Microcontroller

Figure 3.20 shows the Microcontroller IC. Arduino Uno is a microcontroller board based on the ATmega328P [28]. It has 14 digital input/output pins, 6 analog inputs, a 16 MHz quartz crystal, a USB connection, a power jack, an ICSP header and a reset button. In addition, 6 pins out of 14

digital pins can be used as PWM outputs. It contains everything needed to operate the microcontroller. A connection with computer by a USB cable or a AC-to-DC adapter or battery is needed to turn ON the microcontroller. It is a cheap device. "Uno" means one in Italian and was chosen to mark the release of Arduino Software (IDE) 1.0. The Uno board and version 1.0 of Arduino Software (IDE) were the reference versions of Arduino, now evolved to newer releases. The Uno board is the first in a series of USB Arduino boards, and the reference model for the Arduino platform.

Table 2.1 : The Technical Specification of Arduino Uno

Microcontroller	ATmega328P
Operating Voltage	5V
Input Voltage (recommended)	7-12V
Input Voltage (limit)	6-20V
Digital I/O Pins	14 (of which 6 provide PWM output)
PWM Digital I/O Pins	6
Analog Input Pins	6
DC Current per I/O Pin	20 mA
DC Current for 3.3V Pin	50 mA
Flash Memory	32 KB (ATmega328P) of which 0.5 KB used by bootloader
SRAM	2 KB (ATmega328P)
EEPROM	1 KB (ATmega328P)
Clock Speed	16 MHz
LED_BUILTIN	13
Length	68.6 mm
Width	53.4 mm
Weight	25 g

Table 2.1 shows the technical details of Arduino Uno microcontroller. Pull down or up resistances are used to safely operate the microcontroller.

3.4.4 Gate Driver IC TLP 250

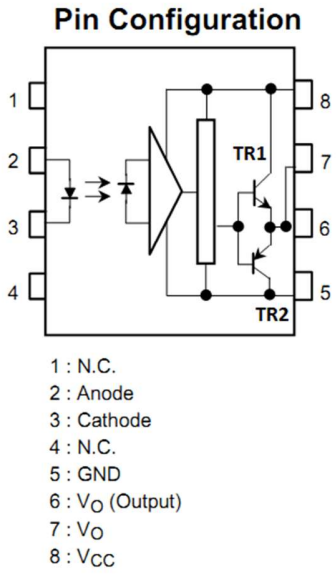

Figure 3.21: The gate driver IC TLP 250

Figure 3.21 clearly shows the input terminals (Pin 2 and 3) LED side and the receiving photodetector as well as the totem-pole driver stage. No connection is needed for Pins 1 and 4, and hence are labeled N.C. meaning no connection.

Pin 8 is VCC – the positive supply. Pin 5 is GND – the ground supply or the return path for the driving power supply. The supply voltage must be at least 10V. The maximum voltage is dependent on the operating temperature. If the temperature is lower than 70°C, up to 30V can be used. For temperatures between 70°C and 85°C, up to 20V can be used. However, there shouldn't be a need to use higher than 20V anyways. In most cases, you'll be using 12V or 15V or perhaps in some cases 18V.

Pins 2 and 3 are the inputs to the LED, anode and cathode respectively. Like regular LEDs, it has an input forward voltage and a peak forward current. The forward voltage will typically be

between 1.6V and 1.8V. The forward current should be less than 20mA. The threshold input current for output transition from low to high is typically 1.2mA, but may be as high as 5mA. Thus, 10mA current should be good.

Even though pins 6 and 7 are shown to be internally connected, the output should be taken from pin 6 as the image - datasheet - shows pin 6 labeled as Vo (Output) []. The output voltage will tend to rise to supply voltage when high (it will actually be slightly lower) and fall to ground level when low.

The TLP250, being an optically isolated driver, has relatively slow propagation delays (not to say that optically isolated drivers can't be fast; there are optically isolated drivers faster than TLP250). The propagation delay time will typically lie between 0.15µs and 0.5µs. An important thing to remember is that the datasheet specifies the maximum operating frequency to be 25kHz.

That covers the different parameters related to TLP250. Now let's go to the design stage and look at a few circuits. One thing mustbe remembered to do when designing circuits with TLP250 is that, a 0.1µF bypass capacitor (ceramic capacitor) should be connected between V+ (pin 8) and V- (pin 5). This capacitor stabilizes the operation of the high gain linear amplifier in the TLP250. Failure to provide this capacitor may impair the switching property. The capacitor should be placed as close to the TLP250 as possible. The closer, the better.

3.4.5 Metal Oxide Semiconductor Field Effect Transistor (MOSFET)

Figure 3.22: MOSFET

A MOSFET may be thought of as a variable resistor whose Drain-Source resistance (typically Rds) is a function of the voltage difference on the Gate-Source pins [29]. If there is no potential difference between the Gate-Source, then the Drain-Source resistance is very high and may be thought of as an open switch, so no current may flow through the Drain to Source pins. When there is a large Gate-Source potential difference, the Drain-Source resistance is very low and may be thought of as a closed switch and current may flow through the Drain-Source pins.

For an N channel MOSFET, the source is connected to ground. If we want to let current flow, we can easily raise the voltage on the gate allowing current to flow. If no current is to flow, the gate pin should be grounded.

P channel – Looking at the P channel MOSFET, the source is connected to the power rail V2. In order to allow current to flow the Gate needs to be pulled to ground. To stop the current flow, the gate needs to be pulled to V2. A potential problem is if V2 is a very high voltage it can be difficult raising the gate to the V2 voltage. Not only that, but the MOSFET has limitations on the Gate-Source potential difference.

Ideally the Drain-Source resistance is very high when no current is flowing, and very low when current is flowing. The main issue using MOSFETs with micro controllers is that the MOSFET may need 10-15 V Gate-Source potential difference to get near its lowest Drain-Source resistance, but the microcontroller may run on 5 V or 3.3 V. Some sort of MOSFET driver is required.

A heat sink on the back of a mosfet is connected to the Drain. To mount multiple MOSFETs on a heat sink, the MOSFET must be electrically isolated from the heat sink. It's good practice to isolate regardless in case the heat sink is bolted to a grounding frame.

The Mosfets also have an internal diode which may allow current to flow unintentionally (freewheeling diode). The body diode will also limit switching speed. This won't be a concern if it is operated below 1 Mhz.

3.4.6 Hall Sensor

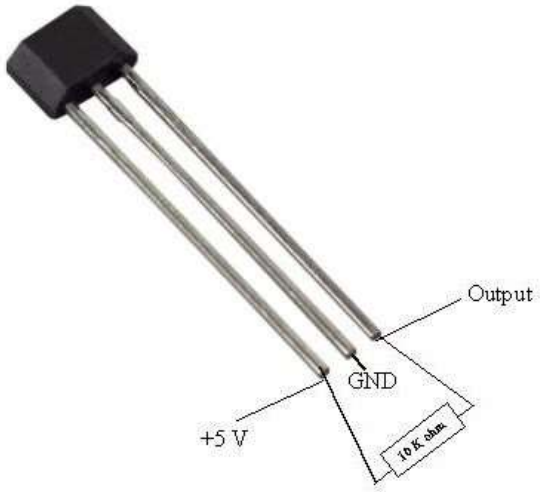

Figure 3.23: Hall Sensor IC [30]

In the Figure 3.23, a Hall sensor IC is given [30]. Hall effect sensors used in brushless DC motors (BLDCs) play a significant role in the reliability, performance and life cycle of many critical applications including robotics, portable medical equipment, HVAC fans and machine tools. These highly efficient motors use hall effect sensors and control circuitry to detect the position of the rotor. Their role is to determine when to apply the current to the motor coils so the electronic controller can rotate the magnet at the right time and orientation. Accurate measurement of the DC motor's position is important because this data is used to produce the maximum amount of torque on the motor shaft, which is a key element of motor efficiency.

As energy efficiency, power consumption and cost savings become bigger design drivers, BLDC motor manufacturers need to adapt to these changing requirements to deliver more efficient motors. This means BLDC motor manufacturers need to carefully consider the bipolar latching hall effect sensor used to commutate the motor. BLDC motors use electronic commutation to control power distribution to the motor, unlike brush DC motors that use mechanical commutation. They should evaluate these sensors based on several technical characteristics, including sensitivity, repeatability and stability over temperature and response time, to ensure that their motor design will operate more efficiently.

Hall effect sensors for BLDCs should provide high repeatability and stability, and a fast response to changes in the magnetic field to deliver greater motor efficiency. Sensor manufacturers have achieved these goals through the use of chopper stabilization, which basically has become a defector standard for hall effect sensors. However, designers should consider new sensor technologies that don't require this technique to achieve higher performance. Because of new technologies and processes, magnetic sensor manufacturers are not only achieving high sensitivity and magnetic stability without using chopper stabilization, they are also delivering better performance.

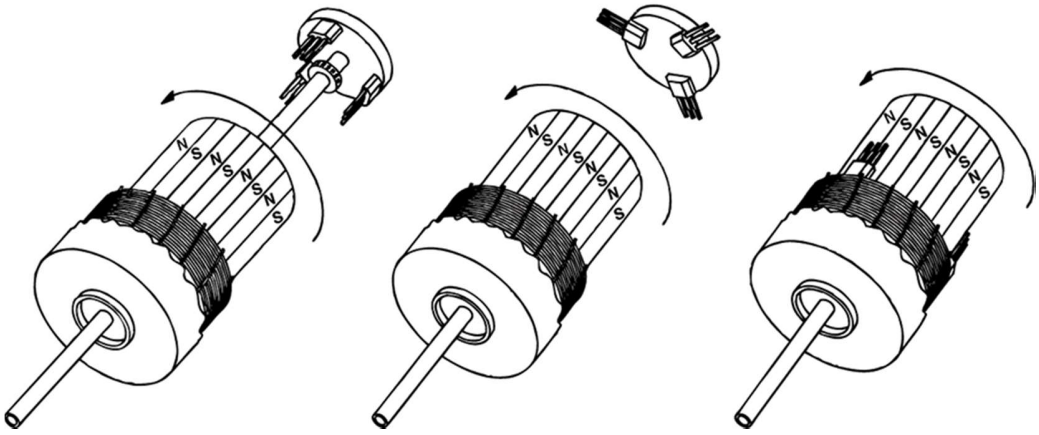

Figure 3.24: The position of Hall Sensor [31]

As seen from Figure 3.24, hall effect sensors can be mounted in one of three locations inside the motor, at the end of the motor's shaft, and around the rotor shaft's ring magnet to measure the motor's position.

3.5 BLDC Motor

Brushless DC motors, rather surprisingly, is a kind of permanent magnet synchronous motor. Permanent magnet synchronous motors are classified on the basis of the wave shape of their induce emf, i.e, sinusoidal and trapezoidal. The sinusoidal type is known as permanent magnet synchronous motor; the trapezoidal type goes under the name of PM Brushless dc (BLDC) machine [21]. Permanent magnet (PM) DC brushed and brushless motors incorporate a combination of PM and electromagnetic fields to produce torque (or force) resulting in motion. This is done in the DC motor by a PM stator and a wound armature or rotor. Current in the DC motor is automatically switched to different windings by means of a commutator and brushes to create continuous motion. In a brushless motor, the rotor incorporates the magnets, and the stator contains the windings. As the name suggests brushes are absent and hence in this case, commutation is implemented electronically with a drive amplifier that uses semiconductor switches to change current in the windings based on rotor position feedback. In this respect, the BLDC motor is equivalent to a reversed DC commutator motor, in which the magnet rotates while the conductors remain stationary. Therefore, BLDC motors often incorporate either internal or external position sensors to sense the actual rotor

3.5.1 Advantages of BLDC motor

BLDC motors have many advantages over brushed DC motors and induction motors. Some of the major points are given:

- Better speed versus torque characteristics
- Faster dynamic response
- High efficiency
- Long operating life
- Noiseless operation
- Higher speed ranges

In addition, the ratio of torque delivered to the size of the motor is higher, making it useful in applications where space and weight are critical factors.

3.5.2 Structure of Permanent Magnet Brushless DC Motor

BLDC motors come in single-phase, 2-phase and 3-phase configurations. Corresponding to its type, the stator has the same number of windings. Out of these, 3-phase motors are the most popular and widely used. Here we focus on 3-phase motors.

- **Stator**

The stator of a BLDC motor consists of stacked steel laminations with windings placed in the slots that are axially cut along the inner periphery. Traditionally, the stator resembles that of an induction motor; however, the windings are distributed in a different manner. Most BLDC motors have three stator windings connected in star fashion. Each of these windings are constructed with numerous interconnected coils, with one or more coils are placed in the stator slots. Each of these windings are distributed over the stator periphery to form an even numbers of poles. As their names indicate, the trapezoidal motor gives a back trapezoidal EMF as shown in Figure 3.25.

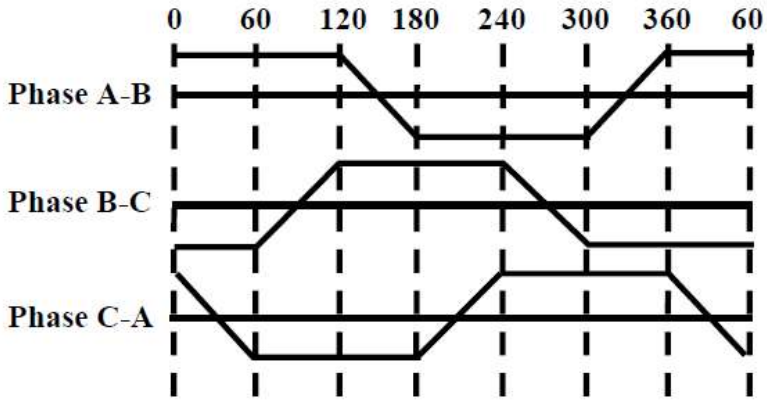

Figure 3.25: Voltage phase diagram of a there phase BLDC motor

In addition to the back EMF, the phase current also has trapezoidal and sinusoidal variations in the respective types of motor. This makes the torque output by a sinusoidal motor smoother than that of a trapezoidal motor. However, this comes with an extra cost, as the sinusoidal motors take extra winding interconnections because of the coils distribution on the stator periphery, thereby increasing the copper intake by the stator windings. Depending upon the power supply

capability, the motor with the correct voltage rating of the stator can be chosen. Forty-eight volts, or less voltage rated motors are used in automotive, robotics, small arm movements and so on. Motors with 100 volts, or higher ratings, are used in appliances, automation and in industrial applications.

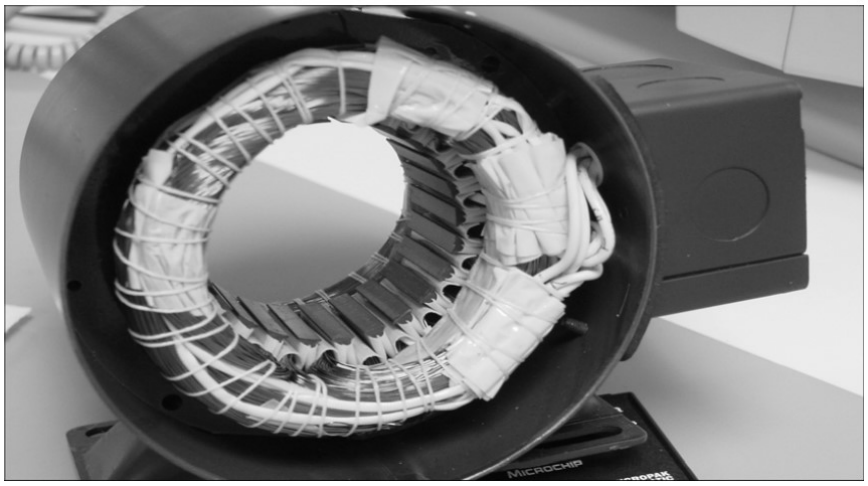

Figure 3.26 : Cross sectional view of the stator

- **Rotor**

The rotor is made of permanent magnet and can vary from two to eight pole pairs with alternate North (N) and South (S) poles. Based on the required magnetic field density in the rotor, the proper magnetic material is chosen to make the rotor. Ferrite magnets were traditionally used to make the permanent magnet pole pieces. For new design rare earth alloy magnets are almost universal. The ferrite magnets are less expensive, but they have the disadvantage of low flux density for a given volume. In contrast, the alloy material has high magnetic density per volume and enables using a smaller rotor and stator for the same torque. Accordingly, these alloy magnets improve the size-to-weight ratio and give higher torque for the same size motor using ferrite magnets. Neodymium (Nd), Samarium Cobalt (SmCo) and the alloy of Neodymium, Ferrite and Boron (NdFeB) are some examples of rare earth alloy magnets. Figure 3.26 shows cross sections of different arrangements of magnets in a rotor.

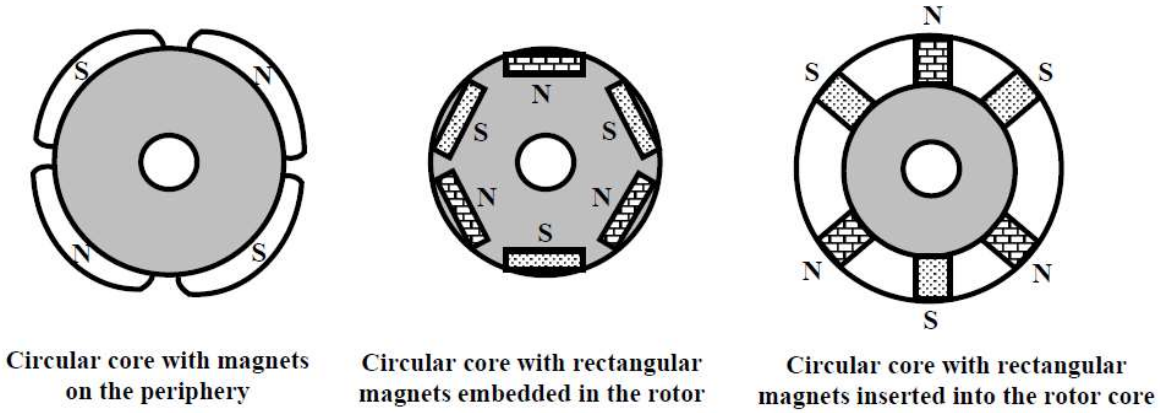

Figure 3.27 : Cross sectional view of different rotor

3.6 Hardware Implementation

This section is introduced to show the hardware implementation of all circuits such as PWM circuit, gate driver and three phase inverter.

3.6.1 Implementing PWM Circuit

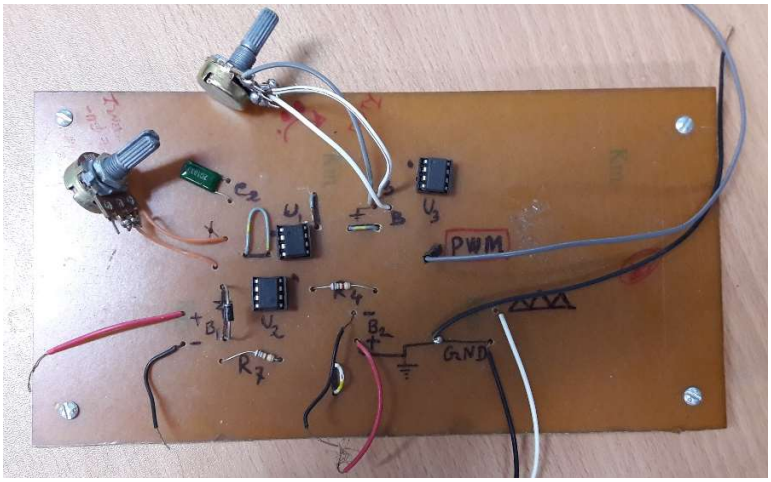

Figure 3.28: Implemented PWM circuit

In the Figure 3.28 shows the PWM circuit that generated required switching signals for the three phase inverter and can be controlled by the potentiometer.

3.6.2 Microcontroller Unit (Arduino Uno)

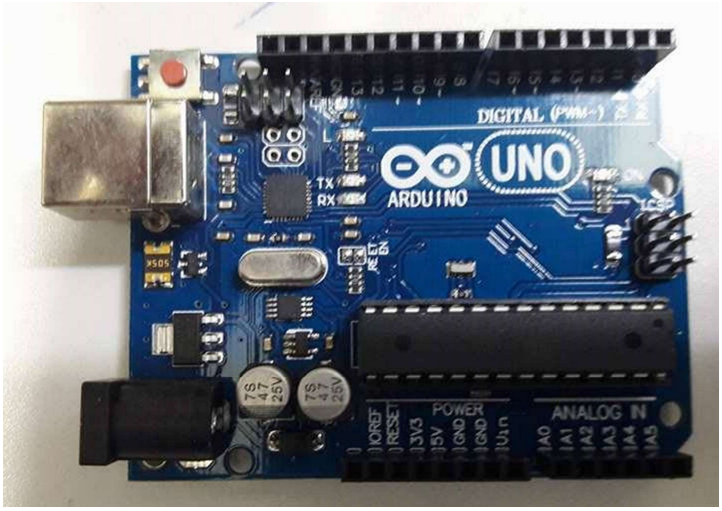

Figure 3.29: Microcontroller Unit (Arduino Uno)

Arduino Uno microcontroller is shown in Figure 3.29. Among 14 pins, 5 pins are coded as inputs and 6 as outputs which goes to the gate driver circuits.

3.6.3 Hardware Design of Gate Driver Circuit

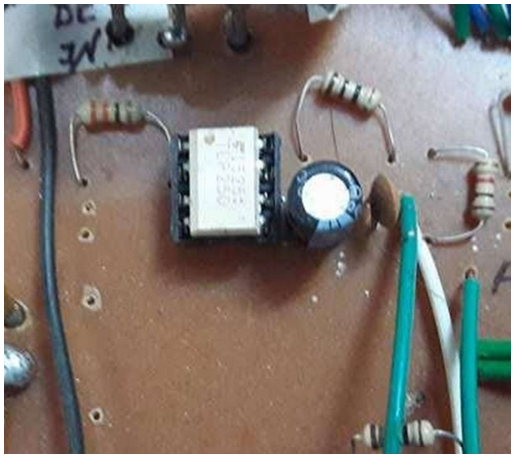

Figure 3.30: Hardware design of the gate driver circuit

Figure 3.30 shows the hardware set up of the one unit of gate driver which provides output to operate the three phase inverter. The circuit is biased using 12 V. It is used for high side and low side switches separately.

3.6.4 Hardware Design of the Three Phase Inverter

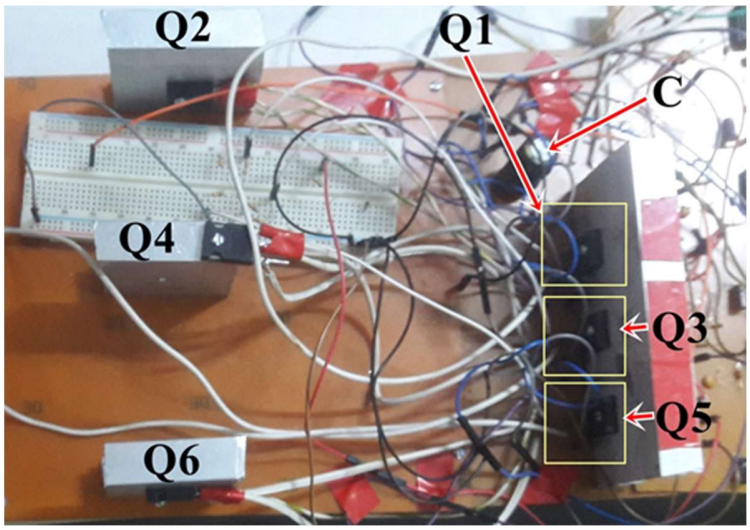

Figure 3.31: The three phase inverter using IRF 250

This is the main power inverter which is used to drive brushless dc motor. The input to the inverter is 48 V and the load (motor) is rated at 500 W. Heat sinks are used to protect the MOSFET (Q1 to Q6) from over heat. All necessary connections are done by soldering.

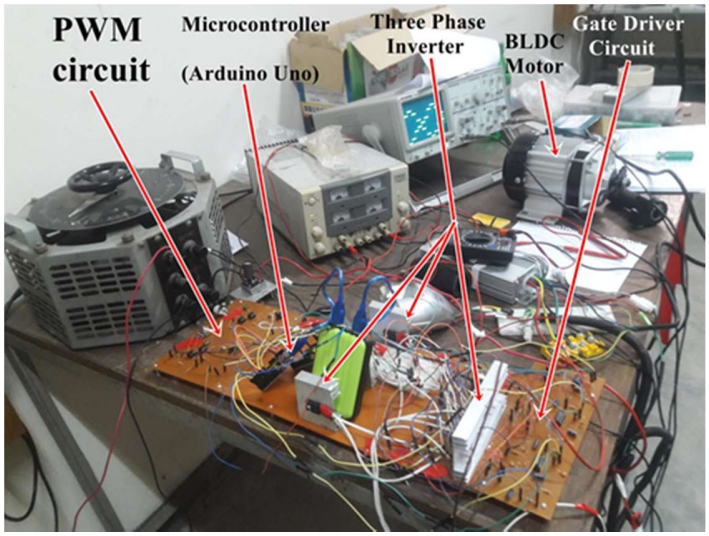

Figure 3.32: Whole hardware setup

Figure 3.32 shows the hardware circuit which is implemented according to described operation. MOSFET (IRF250) is used as switch in this inverter and Arduino uno microcontroller is used to

generate the desired switching pulses. TLP 250 is used as a gate driver circuit. The PWM circuit is implemented using IC741. To vary the pulse width a potentiometer is used. Finally the brushless dc motor is connected with the inverter.

3.7 The Mechanical Structure

In this section, the mechanical structure is designed to store the kinetic energy during motor running operation and hold the motor setup.

3.7.1 The Flywheel

Figure 3.33: The motor and mechanical setup

Figure 3.33 shows the motor including a flywheel. The weight of the flywheel is 10 Kg. This is used to store kinetic energy which will be returned to the supply as electrical energy by the regenerative braking system.

3.7.2 The Overall Setup

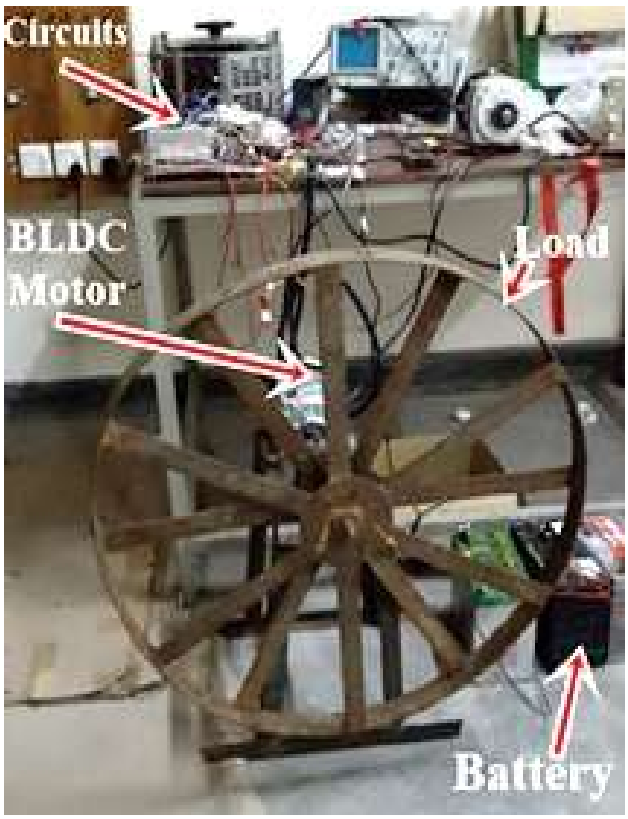

Figure 3.34: The complete set up

The total set of for the research work is depicted in Figure 3.34. Multi cell batteries are used to provide 48 V. The circuit in the figure consists of the previously mentioned parts such as pwm circuit, hall sensors, arduino uno, gate driver and three phase inverter. A brushless dc motor is connected with the three terminals of the inverter. To harness the energy from the braking system, the weight is attached as flywheel.

3.8 PCB Designing

In this section, printed circuit boards for different circuits used in this work will be shown. These layouts will provide the designs of the top copper layer, silkscreen, pads and text on top layer.

3.8.1 PCB Layout for the PWM Circuit

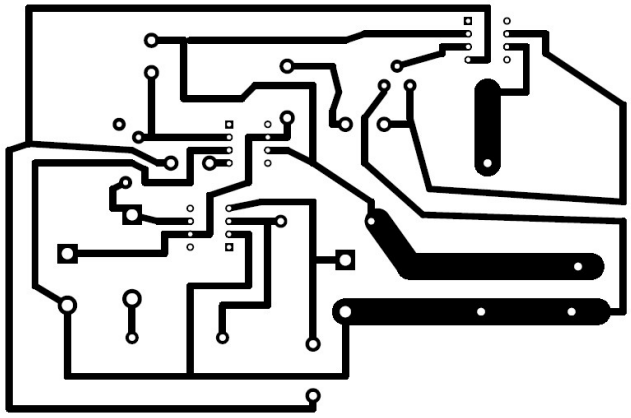

Figure 3.35: PCB layout (top copper layer) of PWM circuit

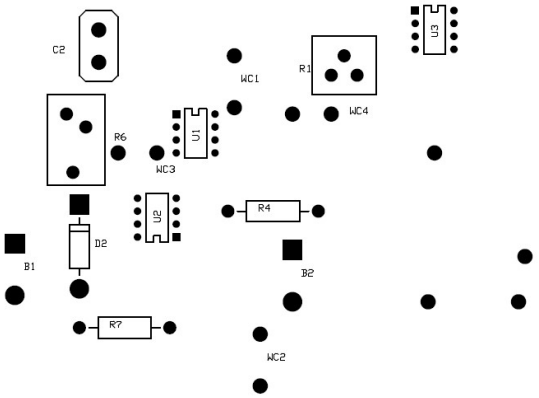

Figure 3.36: PCB layout (silkscreen, pads and text on top layer) of PWM circuit

Figure 3.35 and 3.36 show the PCB layouts for the PWM circuit. Three IC 741 are used and potentiometers are used to vary the frequency and width of the pulse. The layouts are designed in ExpressPCB.

3.8.2 PCB Layout for the Gate Driver Circuit

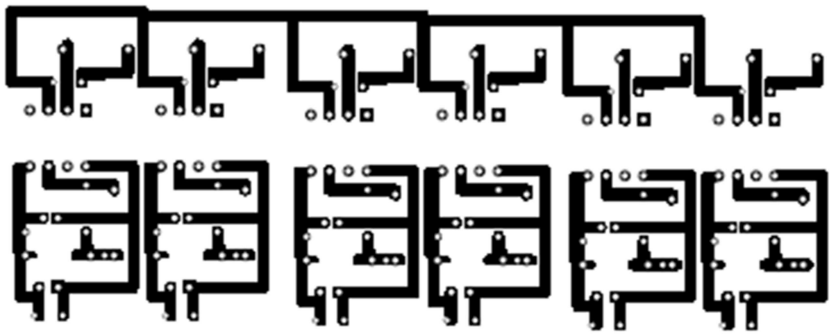

Figure 3.37: PCB layout (silkscreen, pads and text on top layer) of gate driver circuit

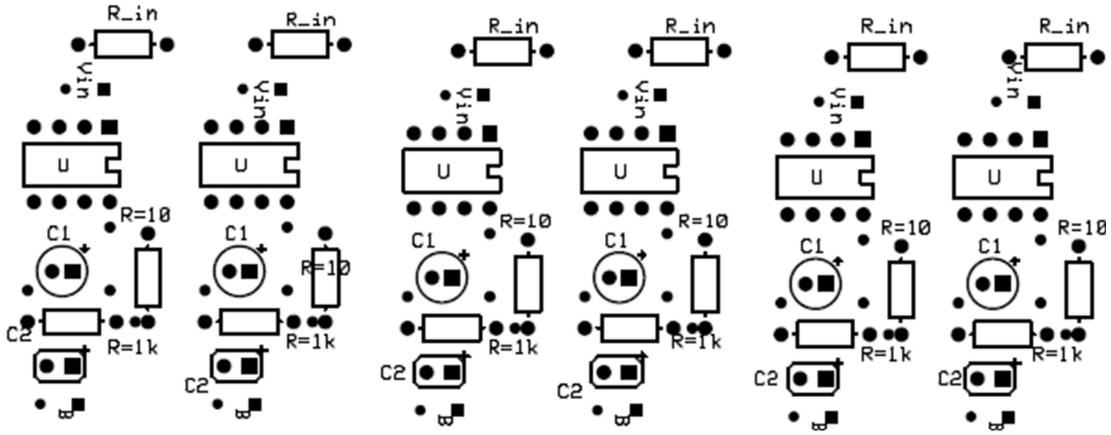

Figure 3.38: PCB layout (silkscreen, pads and text on top layer) of gate driver circuit

PCB layouts for gate driver circuit used in three phase inverter are shown in Figure 3.37 and 3.38 using ExpressPCB. Six gate driver circuits are designed to drive the six mosfets of the inverter.

3.8.3 PCB Layout for the Three Phase Inverter

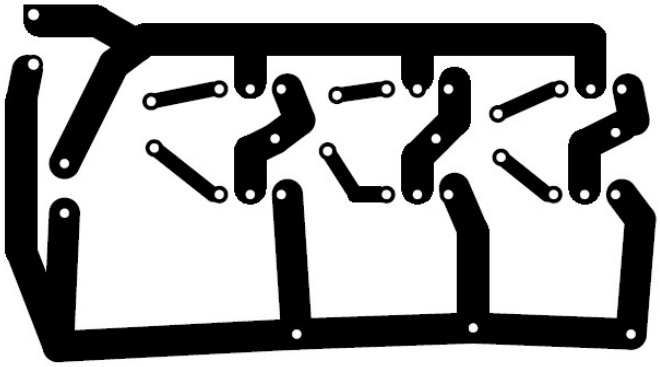

Figure 3.39: PCB layout (silkscreen, pads and text on top layer) of three phase inverter

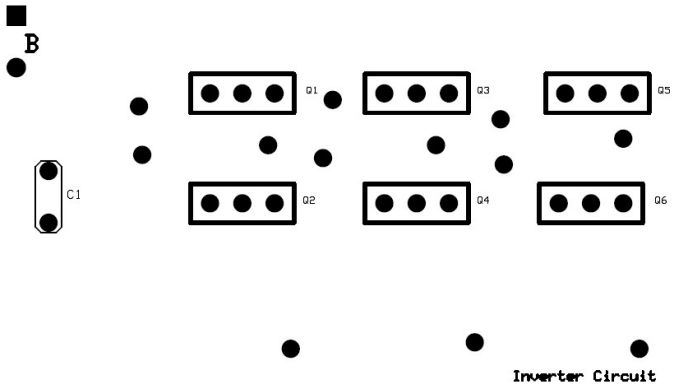

Figure 3.40: PCB layout (silkscreen, pads and text on top layer) of three phase inverter

The top copper layer and silkscreen pads including text on the top layer are shown in Figure 3.39 and 3.40. IRF 250 MOSFET is used in this design. The traces are made thicker considering the current rating of the motor.

3.9 Conclusion

In this chapter wide description about the proposed regenerative braking system is shown. Additionally, the motor operation and inverter design are studied and necessary components for the design are explained. The simulation circuits are depicted and hardware design is done. A flywheel is designed to study the load performance of the system. Finally, the PCB layouts are attached at the end.

Chapter 4

Simulation and Experimental Results

4.1 Introduction

This chapter contains the detail results of the proposed braking systems. At first, the simulation results are discussed, and then the practical results are achieved and compared to the simulated results. The outputs of the microcontroller and the pulse width modulated circuit are shown. After that, the three phase inverter is simulated. Additionally, the three phase inverter outputs are seen from the oscilloscope and successful outcome is obtained. The motor is attached with a weighty flywheel acting as the load. The current readings during the motoring mode and regenerative mode are seen. Finally, the energy regeneration is achieved and calculated.

4.2 Simulated Results

In this section the simulation is done for different parts of the system such as, microcontroller unit, PWM circuit and three phase inverter. The softwares used are PSIM, Protues and Arduino.

4.2.1 Simulated Outputs of the PWM Circuit

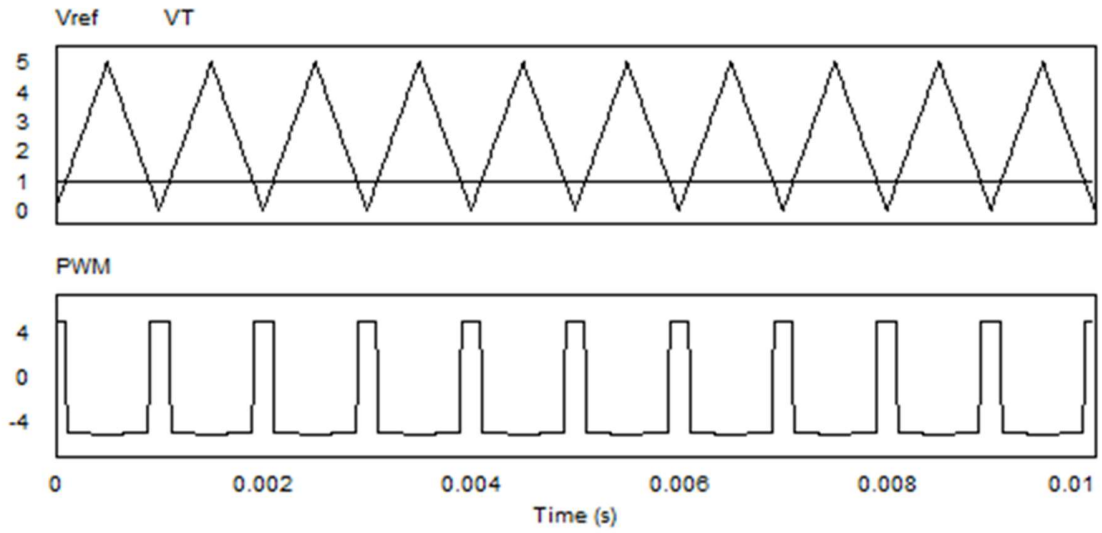

(a)

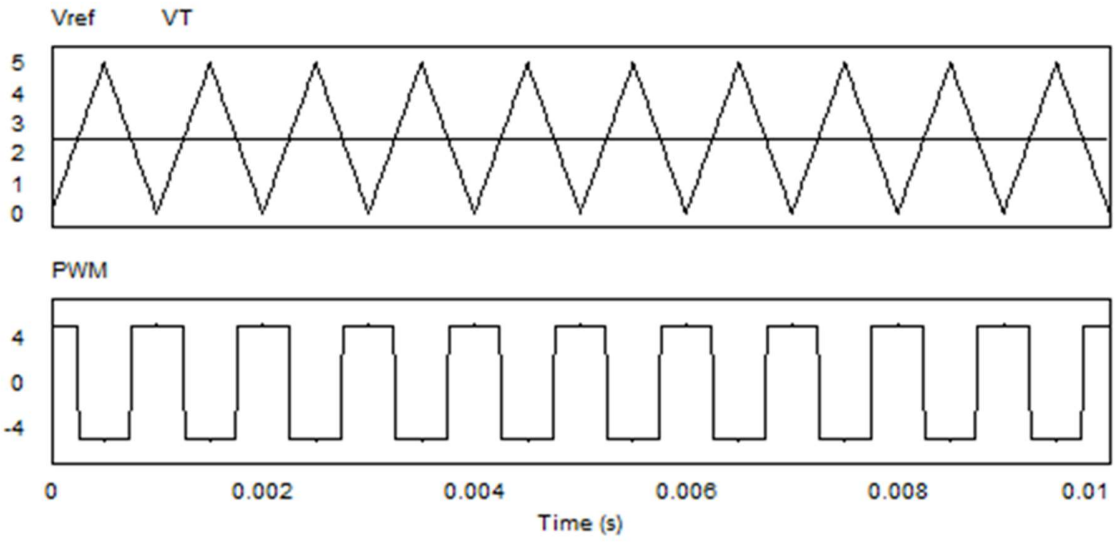

(b)

Figure 4.1: PWM outputs from the simulation

The simulated PWM is shown in Figure 4.1. At first a unipolar triangular wave is generated in the Figure 4.1 (a) . Then, the generated triangular wave is compared with a reference signal to obtain the desired PWM. As seen from the Figure, depending on the reference signal the pulse width is changed. In this case, the width of the pulse is dependent on the height of the reference signal and shows a proportional relationship with the reference voltage. Variable pulse width is required to adjust the output voltage of the three phase inverter which will be noticed during the inverter simulation section.

4.2.2 Simulated Outputs of the Hall Sensor Circuits

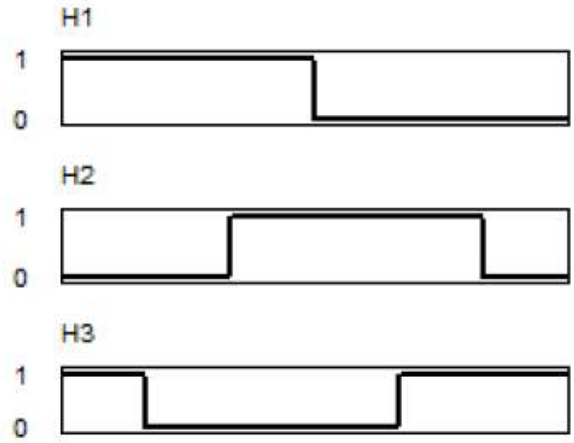

Figure 4.2: Outputs from hall sensors

Figure 4.2 shows the outputs from the hall sensor circuit. When the motor completes its one full rotation, then depending on the number of pole pairs, the outputs are generated. They are 120 degree out of phase and have 50% duty cycle. There are given as input to the microcontroller for producing desired switching patterns.

4.2.3 Simulated Outputs of the Comparator Circuits

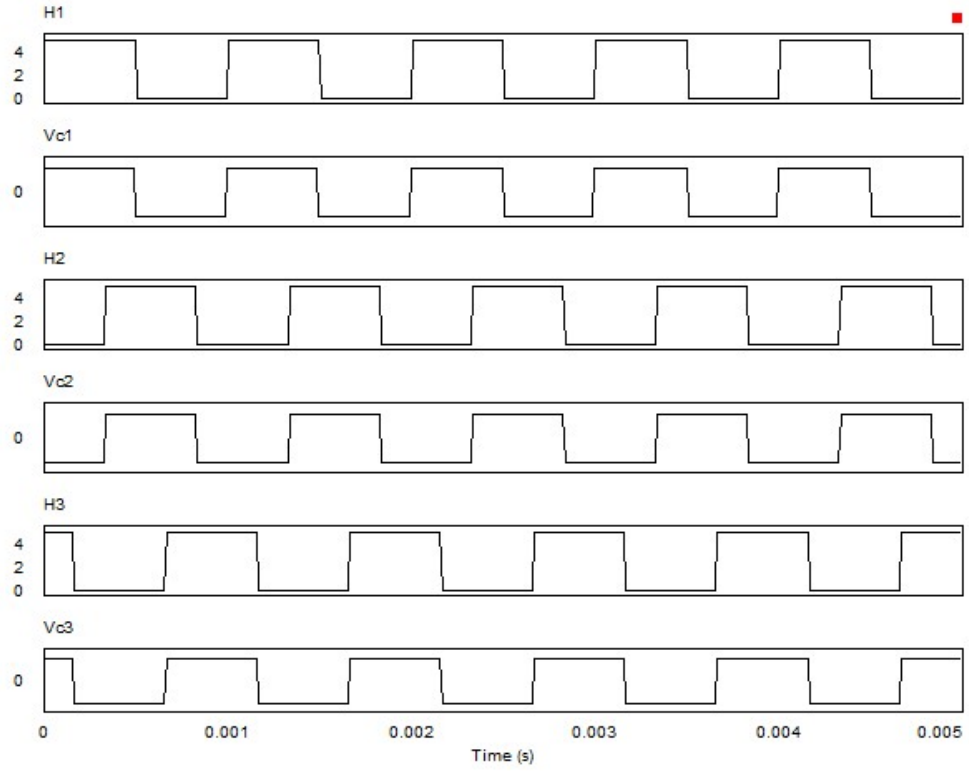

Figure 4.3: Simulated outputs from comparators

Figure 4.3 shows the outputs of three comparators. The inputs are taken from three hall sensor circuits and compared with a 2.5 V source. Doing so yields outputs similar pattern of inputs and avoids direct connections which can interrupt microcontroller`s performance. In this Figure, the inputs are H1, H2 and H3, while the outputs are denoted as Vc1, Vc2 and Vc3. These will be fed into microcontroller.

4.2.4 Simulated Outputs of the Microcontroller

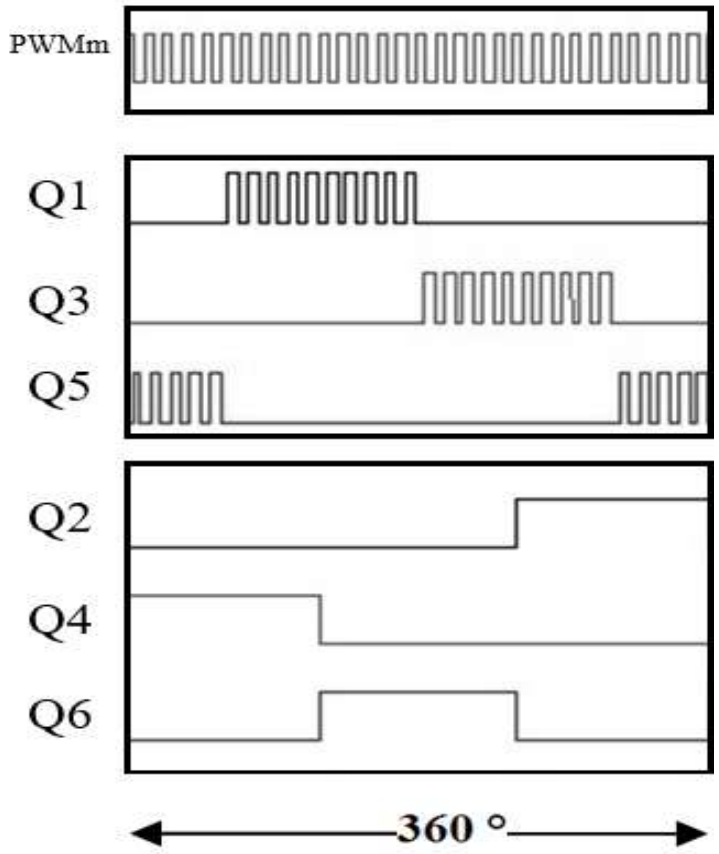

Figure 4.4: Inputs and Outputs of microcontroller

Figure 4.4 shows the inputs and outputs of the microcontroller (Arduino). PWMm is the input to the microcontroller. The desired output pulses Q1 to Q6 are generated by the microcontroller. The result matches with the desired pulses of Figure 3.9. The code for microcontroller is executed in Arduino and the code based output is shown from Proteus simulation.

4.2.5 Simulation of the Three Phase Inverter

Figure 4.5: The switching pulses

The switching pattern shown in Figure. 4.5 is given to the inverter to obtain the desired output voltage from the inverter. This generated swithching pattern is for operating the brushless dc motor and applied to the three phase inverter of Figure 3.17.

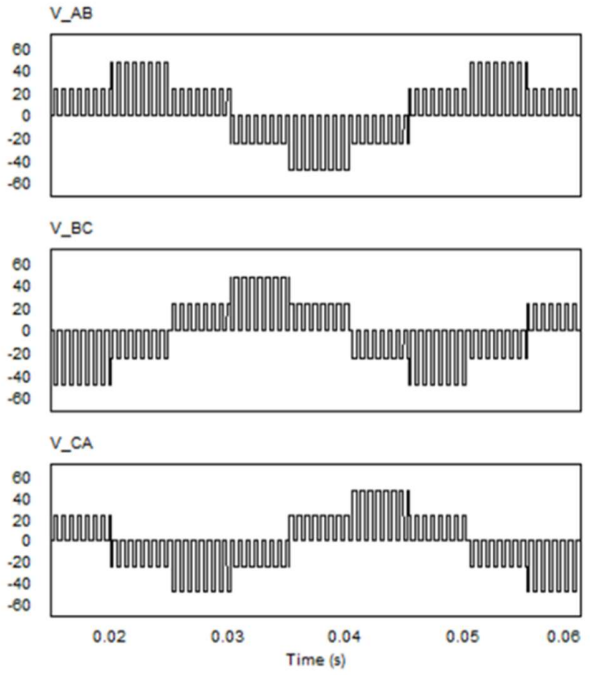

Figure 4.6: The line to line voltages of the three phase inverter

Based on the desired switching shown in Figure 4.4, the simulation has been done in PSIM. The line to line voltages are shown in Figure 4.7. The output voltage of the inverter can be changed to vary the switching pulse width. In this simulation, the pulse frequency is set at 1.5 KHz and the duty cycle is at 50%. Moreover, the battery used has rated voltage of 48 V. The output voltages have a phase difference of 120° and peak voltage of 48 V. The frequency of the inverter is related to the motor`s speed. Increasing the duty cycle to 100% will make the inverter`s output voltage continuous.

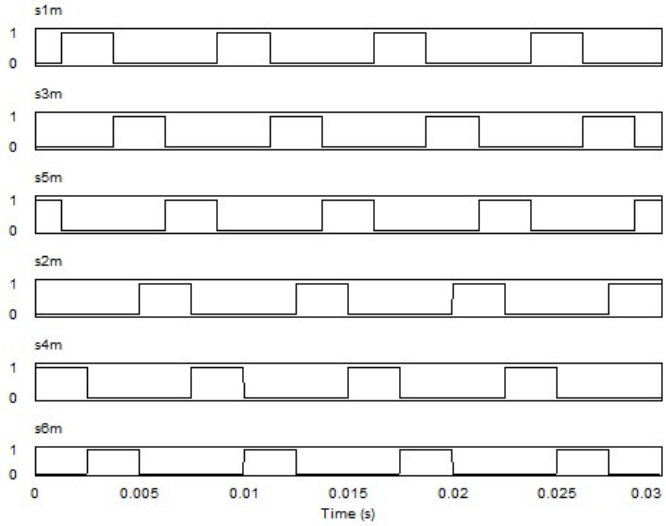

(a)

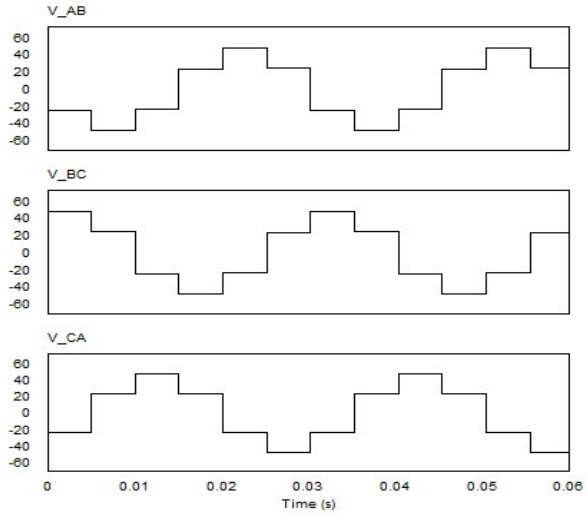

(b)

Figure 4.7: Pulses for 100% duty cycle and outputs of three phase inverter

As previously discussed, the output voltage of three phase inverter for 100% duty cycle is shown in Figure 4.7 (b). The rms value of the output voltage is dependent on the pulse width of the switching signals. Finally, it can be said that, the inverter is a multilevel inverter.

4.3 The Outptuts from the Hardware Implementation

In this section the practical outputs are obtained from all parts of the system such as, microcontroller unit, PWM circuit and three phase inverter. An oscilloscope, digital multimeter and speed meters are used to measure the necessary data.

4.3.1 Outputs from the PWM Circuit

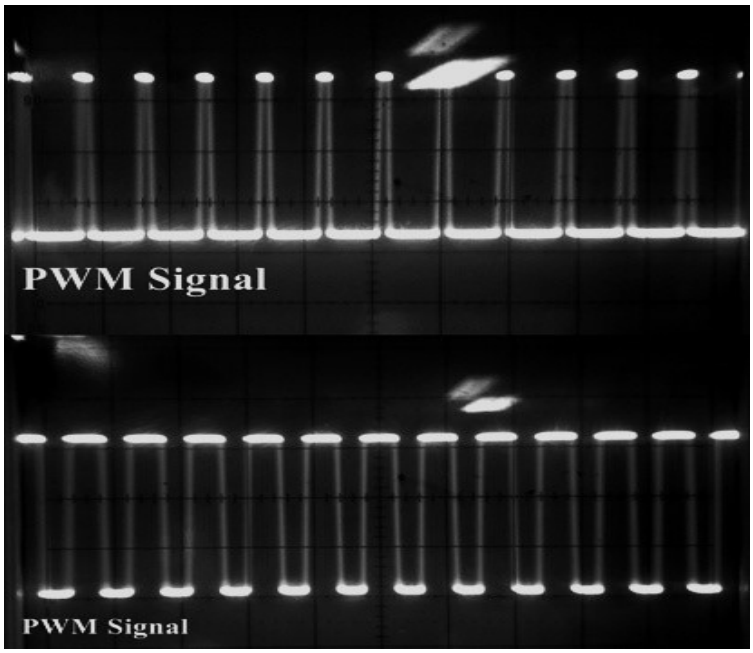

Figure 4.8:Generated PWM signal

Figure 4.8 shows the generated PWM signal. Pulse of varying duty cycle (width) is obtained from the PWM circuit. The upper output has a duty cycle below 50% and the lower one has above 50%. This is done using a variable resistor.

4.3.2 Response of the Hall Circuits

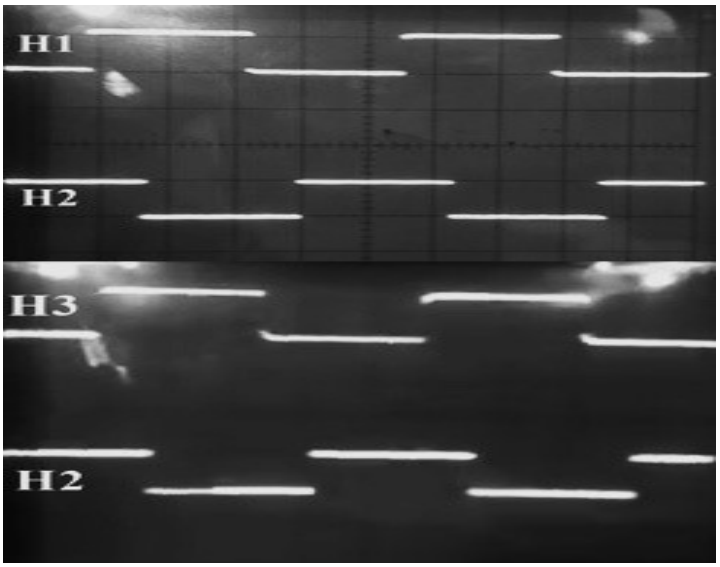

Figure 4.9: The outputs from the hall sensor used in BLDC motor

In the Figure 4.9, the outputs from the hall sensors which are generated during motor rotation and have a peak value of 5 V and 50% duty cycle. The PWM signals having 5V peak and hall signals are given as input to the microcontroller (Arduino Uno), which is coded according to the desired operation.

4.3.3 The Waveforms of Micrcontroller

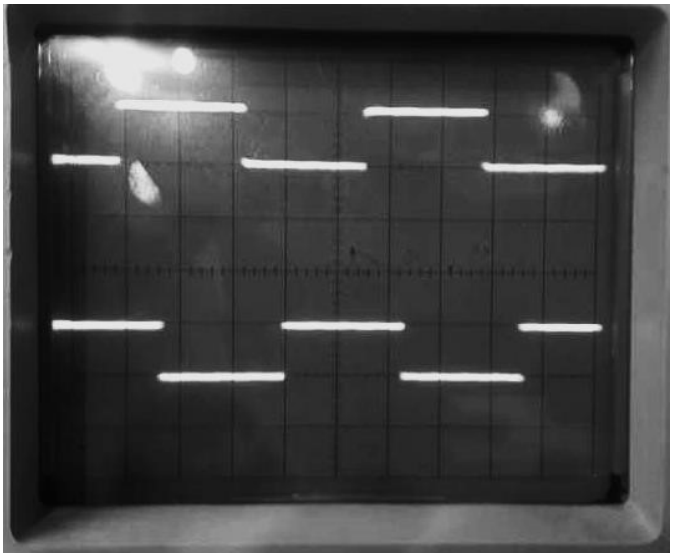

Figure 4.10: The output of Microcotnroller

One particular output from microcontroller is shown in Figure 4.10. The output has 5 V peak. Likewise, other outputs are produced from the microcontroller depending on the pattern of code burnt inside. These outputs will be fed to the mosfet gate driver and are generated for operating the three phase inverter.

4.3.4 The Output Voltages of Three Phase Inverter

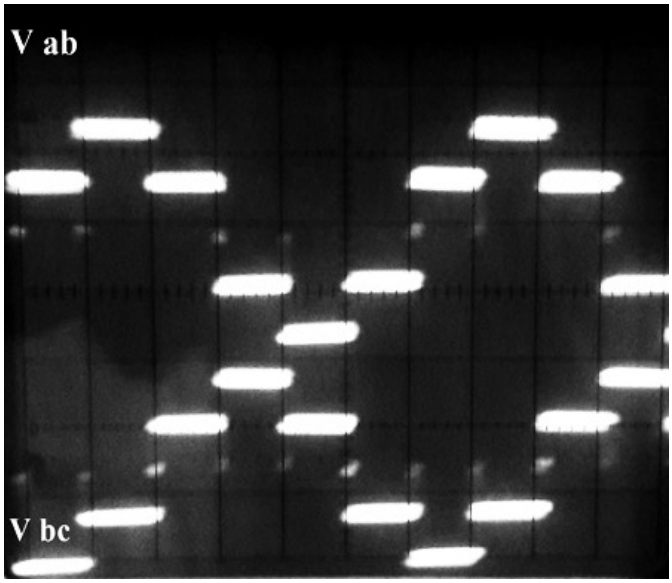

Figure 4.11: Line to line output voltage of the three phase inverter (Vab and Vbc)

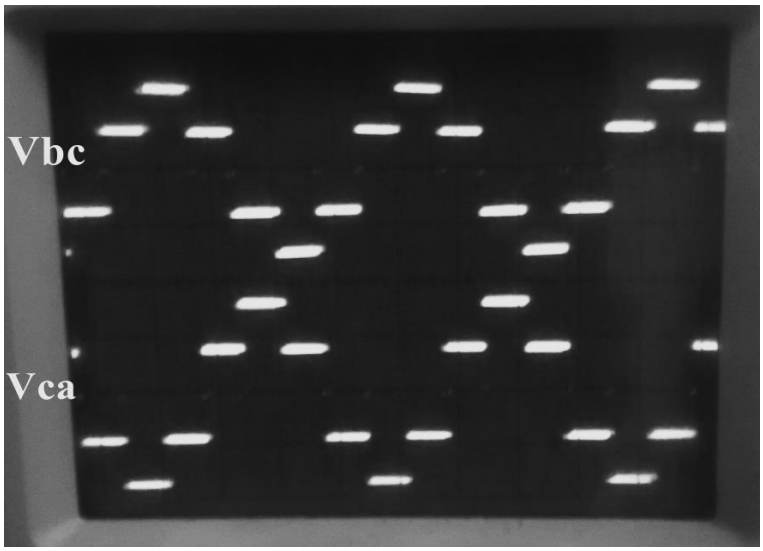

\

Figure 4.12: Line to line output voltage of the three phase inverter (Vbc and Vca)

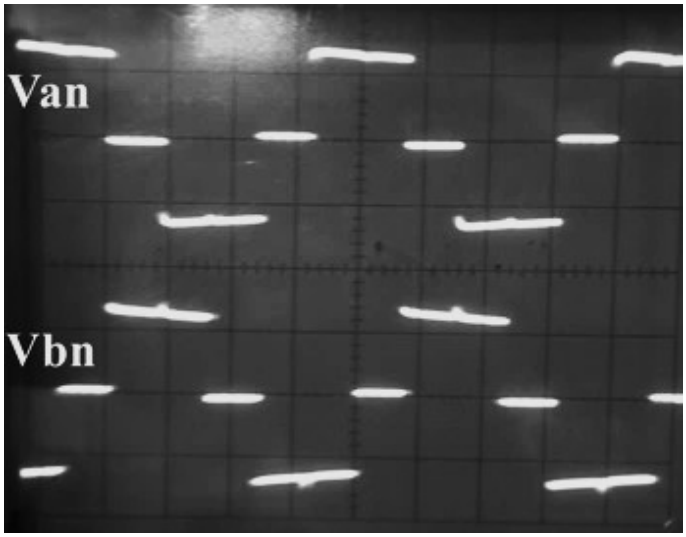

Figure 4.13: Phase voltage of the three Phase inverter (D = 100%)

Figure 4.11 and 4.12 show the line to line voltage of the three phase inverter circuit of Figure 3.31. Likewise**,** the phase voltages of three phase inverter which have 120° difference and peak voltage of around 24 V are shown in the Figure 4.13. All the generated outputs are balanced.The outputs have a perfect match with the simulated outputs shown in the Figure 4.6 and 4.7 .

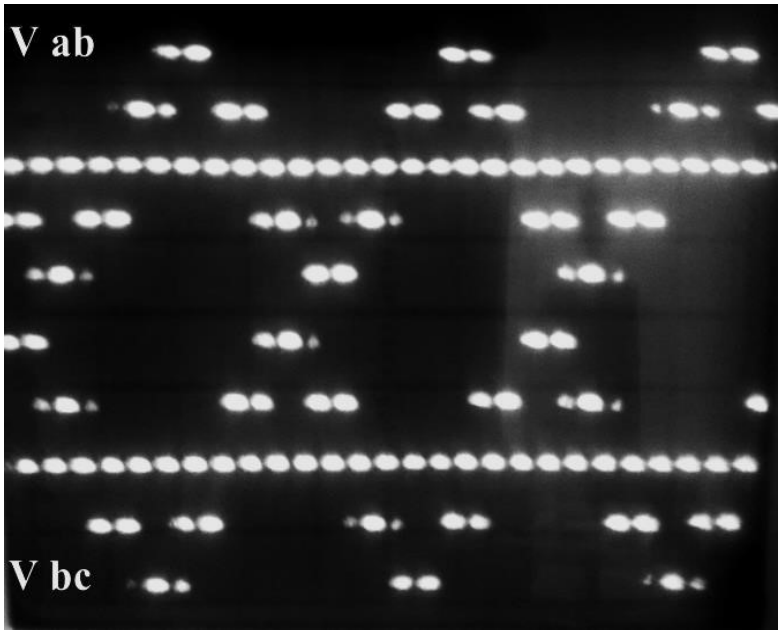

Figure 4.14: Line to line output voltage of the three phase inverter (D = 50%)

The line to line voltage of the three phase inverter is shown in Figure 4.12. The dc input to the inverter is 48 V and the inverter has a peak voltage of 48 V. The output voltage of Fig.14 has been observed depending on a pulse signal of 50% duty cycle. The result exactly matches with the simulated results of Figure 4.6. Output voltage for 100% duty cycle is shown in Figure 4.14. For all the outputs the phase difference is 120°.

4.4 Analysis of the Obtained Data

This section includes the practical data which have been noted from the implemented circuits. In addition, it also provides graphs to illustrate the significance of the gathered data. Energy regeneration, back emf and speed at different duty cycles have been recorded to provide an estimate for future development.

4.4.1 Inverter Output and Motor Speed

Table 4.1: Inverter Output Voltage and RPM of the Motor

Serial	Duty Cycle	Inverter Output Voltage (V_{LL})	Speed
1	85%	31.2 V	448 rpm
2	70%	28.5 V	400 rpm
3	60%	26.2 V	367 rpm
4	40%	21.7 V	300 rpm
5	30%	18.1 V	250 rpm

Table 4.1 shows the motor speed for different inverter voltage. The frequency of the switching pulse is set at 1.5 KHz. The speed has a proportional relation with the duty cycle or the applied voltage.

Figure 4.15: The running motor

Figure 4.15 shows the successful running operations of motor. The ratings of the motor used in this research are 500 W and 48 V. The motor is connected with the inverter circuit and the pulse width is changed to vary the speed. The speed for different voltage has been noted using a laser tachometer.

4.4.2 Back EMF and Motor Speed

It is already mentioned that, the back emf produced in the motor is sinusoidal in nature. Thus, a rectified dc is obtainable during motor shut down operation across the battery terminals. The magnitude of rectified back emf is measured at different speeds.

Table 4.2: Duty Cycle, Speed and Rectified Back EMF of the Motor

Serial	Duty Cycle (%)	Speed (rpm)	Rectified Back EMF (V)
1	12.5	129	10.00
2	16.5	157	15.34
3	22.5	209	16.37
4	24	224	20.36
5	29	241	22.11
6	33	267	23.17
7	36	284	24.46
8	41	290	25.37
9	56	325	27.00
10	63	339	30.00
11	75	353	31.5

The change of speed and back emf (Rectified) is measured in terms of different duty cycle adjusted by the potentiometer of the PWM circuit. Table 4.2 reflects a proportional relationship between the specified parameters.

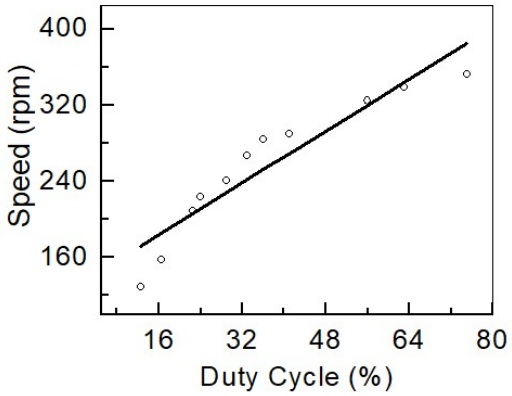

Figure 4.16: RPM of the motor versus duty cycle

Figure 4.16 illustrates the data relating the pulse width (%) of switching signal with the motor`s speed and shows a proportional relationship, which is certainly expected. The speed increase with the increment in duty cycle.

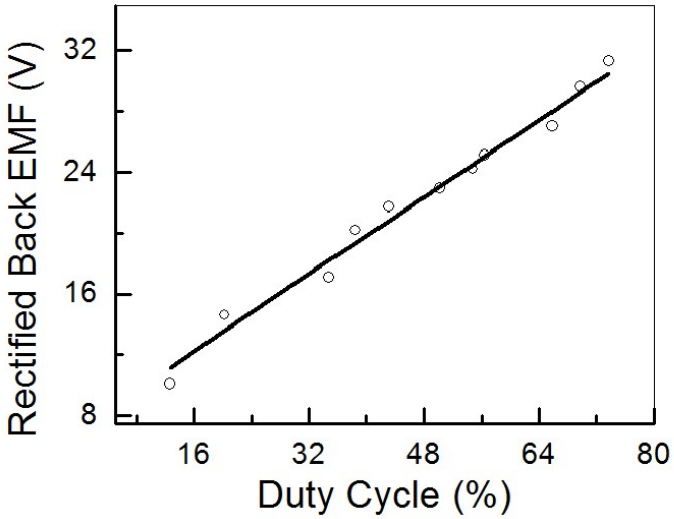

Figure 4.17: Rectified back emf of the motor versus duty cycle

Likewise, another proportional change is seen in Figure 4.17, which reflects the relation between the back emf which is rectified and duty cycle of the switching signals. Both of the characteristics given in Figure 4.16 and 4.17, shows a similar pattern.

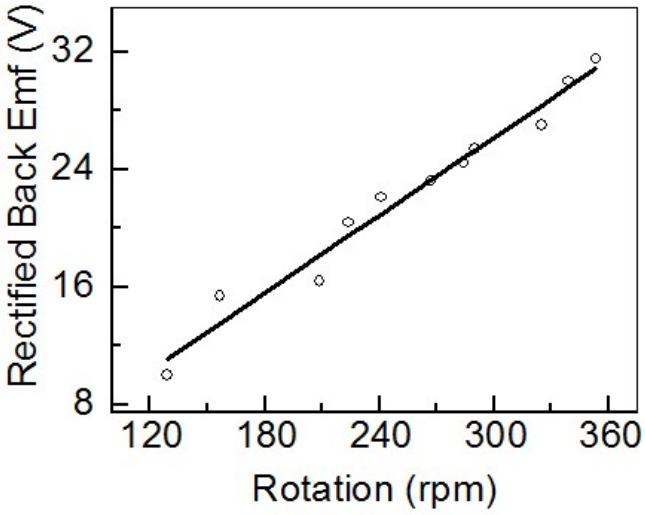

Figure 4.18: Rectified back emf of the motor versus rpm

Based on the data collected in Table 4.2, another graph showing the positive relation between RPM and rectified back emf is given in Figure 4.18. This data are useful to select proper braking systems which will be discussed in the later sections.

4.4.3 Braking Parameters During Regeneration

Table 4.3: Time Parameters During Different Braking Schemes and Braking System

Serial	RPM	Rectified Back EMF (V)	Maximum Braking Current (A)	T_o (Sec)	T_{off} (Sec)	T_{br} (Sec)	Braking System (V)
1	129	10	0	N/A	N/A	N/A	N/A
2	157	15.34	3	2	15	20.5	12
3	209	16.37	3	2	16.5	23	12
4	224	20.36	7	3	16	22.1	12
5	241	22.11	8	3.5	16.5	22.5	12
6	267	23.17	11	4	17	24	12
7	277	25.37	12	5	17.5	27	12
8	325	27	3	2	26	31	24
9	339	30	5	3	27	34	24
10	353	32	6	3	29	36	24

Table 4.3 shows the data obtained from the motor turn off experiment by both normal and regenerative braking scheme and braking system selection. Here, T_o is the time duration for reaching zero current (Sec), $T_{off}$is the time motor takes to become off during regenerative braking (Sec) and T_{br} is the time motor takes to become off during normal braking (Sec).

Selecting an appropriate braking system is dependent on the magnitude of rectified back emf, which is measured across inverter`s input terminals. It is again noted that, an inverter can act as a rectifier in the opposite direction. To justify the data analysis, it is mandatory to observe the rectified back emf which determines the braking system that can be selected from a multi cell battery system. The braking system (at the left column of the table) is selected following the previous discussion and the time is simultaneously monitored. As seen from the table that, as rpm increases the back emf and maximum braking current go up. The analysis also includes the time duration by which the current becomes zero. To charge 24 V battery system, the back emf must be greater than 24 V. Hence, the 24 V braking system is selected from 325 rpm considering the magnitude of back emf, while the 12 V braking system is taken for speed a speed range between 157 and 277 rpm. Moreover, braking times for both normal and regenerative braking are compared and found lower in case of regenerative braking.

Table 4.4: The Motor Current at Different Speeds

Serial	Speed (rpm)	Current (A)	Power Consumption (W)	The Watt-hour for10 Minutes Operation
1.	129	1.23	59.04	9.84
2.	157	1.52	72	12
3.	209	2.48	119.52	19.92
4.	224	4.17	200	33.33
5.	241	4.61	221.28	36.88
6.	267	5.3	256.8	42.8
7.	277	5.65	271.2	45.2
8.	325	7.1	340.8	56.8
9.	339	7.43	355.2	59.2
10.	353	8.1	388.8	64.8

The motor currents at different speeds are noted in the Table 4.4. The current has a proportional relationship with the speed. Power consumptions for different speeds are calculated considering the battery voltage of 48 V. Moreover, energy consumed for a 10 minute interval is calculated to find out the Wh for various mentioned speeds. An upward trend is seen in the watt-hour data for increasing speeds.

Table 4.5: The Energy Regeneration Analysis

Serial	Speed (rpm)	Effective Charging Voltage (V)	Effective Charging Current (A)	Charging Time (s)	Generated Watt-hour Per Cycle	Watt-hour for 20 Cycles
1.	157	13.67	1.5	2	0.0114	0.228
2.	209	14.19	1.5	2	0.0118	0.236
3.	224	16.18	3.5	3	0.047	0.94
4.	241	17.05	4	3.5	0.066	1.32
5.	267	17.56	5.5	4	0.107	2.17
6.	277	18.69	6	5	0.156	3.12
7.	325	25.5	1.5	2	0.021	0.42
8.	339	27	2.5	3	0.056	1.12
9.	353	28	3	3	0.07	1.40

The Table 4.5 shows the energy regeneration data for different speeds. The charging voltage and current are calculated from the back emf data of Table 4.3 and battery voltage. For instance, at a particular speed of 157 rpm, the rectified back emf is 15.34 V that can charge one unit of 12 V battery. So, the effective voltage is (15.34+12) / 2 V or 13.67 V. Likewise, the charging current was monitored and the effective value is calculated. In addition, the charging time data are taken from the Table 4.3 to calculate the generated watt-hour per cycle data in the Table 4.5. Finally,

the number of braking cycles is considered as 20 and corresponding energy regeneration in terms of Watt-hour is calculated to show the overall performance. The braking cycle is selected as 20 from the regular rickshaw visit experience.

At this point, it is important to note that, the experiment is performed using a 10 Kg wheel. In practical cases, the passengers` weight will obviously be higher than the wheel used in this test. The higher the weight, the higher will be the moment of inertia as the relation between the mentioned parameter is proportional. Hence, the generated energy will be higher than the test result. The regenerative braking will certainly decrease electricity consumption for charging the battery from supply and will charge the battery on the go while running on the road.

4.4.4 Results Reflecting the Back EMF Response With Time

This section shows the variation of the rectified back emf with the time. The motor is run at the maximum speed (Around 450 rpm), and then the supply is removed to observe the back emf performance under the loaded condition. The observation is done for a 40 Sec period and recorded in the Table 4.6.The back emf decreases with the time. The maximum back emf at the highest speed of 450 rpm is 33 V.

Table 4.6: Time Versus Rectified Back EMF

Time (Sec)	Back emf (V)	Time (Sec)	Back emf (V)
1	33	21	14.1
2	32.1	22	13.02
3	31.19	23	12.39
4	30.5	24	11.94
5	30	25	11.15
6	28.73	26	10.02
7	26.66	27	9.24
8	26.04	28	8.17
9	25.41	29	7.79
10	24.65	30	7.52
11	23.05	31	7.1
12	22.26	32	6.54
13	21.34	33	5.96
14	20.56	34	5.38
15	19.27	35	4.65
16	18.01	36	4.03
17	17.52	37	3.4
18	16.26	38	2.9
19	15.23	39	2.51
20	14.49	40	1.169

4.5 Cost Analysis

In this section the cost associated with the laboratory circuit construction will be analyzed for the inverter construction and boost converter. After, that the cost effectiveness of the proposed system will be illustrated.

4.5.1 Cost of The Inverter

A three phase inverter consists of six switches (MOSFET), heat sink, capacitor and gate driver circuits. The cost of these components is given in the Table 4.7. Total cost for the three phase inverter construction is 673 Taka.

Table 4.7: Cost of the Inverter

Item	Unit Price (Taka)	Price for all units (Taka)
MOSFET	50	50*6 = 300
Gate Driver IC	50	50*6 = 300
Heat Sink	10	10*6 = 60
Capacitor	13	13*1=13
Total		673

4.5.2 Cost of The Boost Converter

A boost converter consists of one switch (MOSFET), heat sink, gate driver circuits, inductor and capacitor. The cost of these components is given in the Table 4.7. To construct a boost converter in laboratory premises, the amount needed is 183 Taka.

Table 4.8: Cost of the Boost Converter

Item	Unit Price (Taka)	Price for all units (Taka)
MOSFET	50	50*1= 50
Gate Driver IC	50	50*1 = 50
Heat Sink	10	10*1 = 10
Capacitor	13	13*1=13
Inductor	60	60*1=60
Total		183

As the conventional regenerative braking system includes a boost converter with the three phase inverter, the total cost for the traditional system in the laboratory is, (673 +183) Taka = 856 Taka. But in the proposed system, the boost converter is avoided for achieving the cost effectiveness. Hence, the cost is basically limited to 703 Taka (The cost of the braking switch is 30 Taka and included here). The percentage of cost saving is given below:

$$\% \text{ Cost Saving} = \frac{(856 - 703)}{856} * 100\% = 17.87\ \%$$

As a result, it can be stated that, the proposed system is 17.87 % cost effective if compared with that of the conventional regenerative braking system.

4.6 Conclusion

In this chapter, all the results are discussed. This chapter is divided into two major parts containing simulated outputs and practical outputs. All parts of the systems such as PWM circuit, microcontroller, gate driver and inverter are simulated and then from the hardware the real data are obtained and compared. The energy regeneration is calculated at different speeds. Finally, a cost calculation is done to compare the cost effectiveness.

Chapter 5

Conclusion

5.1 Conclusion

In this thesis a cost effective regenerative braking system for low cost electric vehicle is developed. Recently, the vehicle system prefers a brushless DC motor for some lucrative features such as, electronic commutation, noiseless operation and etc. The current system does not include regenerative braking, which stores energy during. Additionally, some systems, including this feature use boost converter that increases the cost and the size of the overall system. Hence, a flexible technique, avoiding the use of boost converter is proposed and experimentally verified. In the first chapter the motivation and overview have been discussed to illustrate the reason of the thesis. A clear and broader discussion is given to point out the drawback of the conventional braking system and cost. Although, a small amount of energy is utilized, but that particular regeneration is worthy as it eliminates the energy wastage that takes place in the traditional braking system. The proposed system and different components used to develop the system are discussed. In addition, an overall idea of the system and the operation of the different units are depicted. After that, every component used in the implementation is presented with their basic characteristics and operation.

The research firstly focuses on the simulated results of the three phase inverter that is the main unit of motor control system. The simulation is based on the desired switching pulses and performed in two different parts such as, first part describe the pulse generation by the microcontroller unit and then the inverter output is seen. Moreover, the necessary pulse width modulated signal that controls the speed is generated. Next, the hardware implementation commences following the simulation. Particularly, every unit associated with the simulation

circuitis designed including the gate driver circuit. Each of the units is separately tested and the motor is operated. To justify the load behavior of the motor a flywheel is arranged. The speeds at different duty cycle of PWM signal are noted and then using the rectifier that exists on the opposite side of a three phase inverter, the generated three phase sinusoidal back emf is rectified to charge the battery. In particular, one switch like a single pole double throw is used to change the operating modes. Finally, braking current at different speeds and the braking current time are noted. The regenerative braking will certainly decrease electricity consumption for charging the battery from supply and will charge the battery on the go while running on the road.

5.2 Future Work

The regenerative braking system is experimentally verified in the laboratory. Moreover, the necessary data are gathered at fixed loaded condition, while real scenario will be different as the loads will be variable at different cases. Additionally, this analysis is done for the motor used in electric rickshaw. However, in future, the analysis of motor of different higher rated vehicle can be carried out based on the proposed research work. Particularly, it can be made commercially available to harness the braking energies in a greater extent. Hence, the exploration of this work at commercial aspect will be a lucrative area of research.

References

[1] Long, B., Lim, S. T., Ryu, J. H., and Chong K. T., "Energy-Regenerative Braking Control of Electric Vehicles Using Three-Phase Brushless Direct-Current Motors," Energies, vol. 7, pp. 99-114, January 2014.

[2] Nian, X., Peng, F., and Zhang, H., "Regenerative Braking System of Electric Vehicle Driven by Brushless DC Motor," IEEE Transactions on Industrial Electronics, vol. 61, issue 10, pp. 5798 – 5808, Oct. 2014.

[3] Lu, S., Corzine, K. A., and Ferdowsi, M., "A new battery/ultracapacitor energy storage system design and its motor drive integration for hybrid electric vehicle, " IEEE Trans. Veh. Technol., vol. 56, no. 4, pp. 1516-1523, Jul. 2007.

[4] Ortuzar, M., Moreno, J., and Dixon, J., "Ultracapacitor-based auxiliary energy system for an electric vehicle: Implementation and evaluation," IEEE Trans. Ind. Electron., vol. 54, no. 4, pp. 2147-2156, Aug. 2007.

[5] Lu, S., Corzine, K. A., and Ferdowsi, M., "A unique ultracapacitor direct integration scheme in multilevel motor drives for large vehicle propulsion," IEEE Trans. Veh. Technol., vol. 56, no. 4, pp. 1506-1515, Jul. 2007.

[6] Sagar Maliye, "Regenerative Braking and Anti-Lock Braking System in Electric Vehicles," M.S. thesis, Dept. Electron. Eng., National Institute of Technology, Odisha, India, 2014.

[7] Rian, M. Z., and Rahman , A. N. M. M., "Study on Power Consumption and Social Aspects of Battery Operated Auto-rickshaw," International Conference on Mechanical, Industrial and Energy Engineering, pp.1-5, Dec. 2014.

[8] P.B. Bobba and K.R. Rajagopal, "Compact regenerative braking scheme for a PM BLDC motor driven electric two-wheeler,"in 2010 Joint International Conference on Power Electronics, Drives and Energy Systems (PEDES) & 2010 Power India, Dec. 2010, pp. 1-5.

[9] M.K Yoong, Y.H. Gan, G.D. Gan, C.K. Leong, Z.Y. Phuan, B. K. Cheah and K.W. Chew, “Studies of regenerative braking in electric vehicle,” in 2010 IEEE Conference on Sustainable Utilization and Development in Engineering and Technology (STUDENT), Nov. 2010, pp. 40-45.

[10] A. Lahyani, P. Venet, A. Ouermazi, and A. Troudi, "Battery super capacitors combination in un interruptible power supply (UPS)," IEEE Transactions on Power Electronics, vol. 28, pp. 1509- 1522,2013.

[11] A. Kuperman, I. Aharon, S. Malki, and A, Kara, "Design of a semi active battery-ultracapacitor hybrid energy source," IEEE Transactions on Power Electronics, vol. 28, pp. 806-815,2013.

[12] N. L. Hinov, D. N. Penev, and G. I. Vacheva , “Ultra Capacitors Charging by Regenerative Braking in Electric Vehicles,” In Proc. XXV International Scientific Conference Electronics - ET2016, September 12 - 14, 2016, pp. 1-4.

[13] Alex C. Bronstein, “Ultra-Capacitor Based Electric Bicycle Regenerative Braking System,” B.S. thesis, Dept. Electron. Eng., California Polytechnic State Univ., San Luis Obispo, United States, 2012.

[14] M. Michalczuk, B. Ufnalski, L. Grzesiak, "Fuzzy logic control of a hybrid battery-ultracapacitor energy storage for an urban electric vehicle", Ecological Vehicles and Renewable Energies (EVER) 2013 8th International Conference and Exhibition on, pp. 1-7, 2013.

[15] V. Sindhuja and G. Ranjitham, “Regenerative Braking System of Electric Vehicle Driven By BLDC Motor Using Neuro Fuzzy and PID,” International Journal of Innovative Research in Science, Engineering and Technology, Vol. 3, Issue 12, pp. 17847 17854, Dec. 2014.

[16] R. Elavarasi and P. K. SenthilKumar, “An FPGA based Regenerative Braking System of Electric Vehicle Driven by BLDC Motor,” Indian Journal of Science and Technology, Vol 7(S7), pp. 1-5, Nov. 2014.

[17] Plaudit Techno India Pvt. Ltd., “Important Factors about Construction and Working of E-Rickshaw,” *Plaudit Techno India Pvt. Ltd.,* 2017. [Online]. Available: http://www.plauditerickshaw.com/e-rickshaw/important-factors-construction-working-e-rickshaw/. [Accessed: Mar. 12, 2017].

[18] Om Balajee Automobile, "E Rickshaw Specification," *Om Balajee Automobile*, 2005. [Online]. Available: http://www.dmwevehicles.com/e-rickshaw.html. [Accessed: Mar. 10, 2017].

[19] D. Torres, and P. Heath, "Regenerative Braking of BLDC Motors," High-Performance Microcontroller Division Microchip Technology Inc., 2015. [Online]. Available: http://eacaspian.ir/wp-content/uploads/2015/06/EB1.pdf [Accessed: May 24, 2016].

[20] N. L. Hinov, D. N. Penev, and G. I. Vacheva , "Ultra Capacitors Charging by Regenerative Braking in Electric Vehicles," In Proc. XXV International Scientific Conference Electronics - ET2016, September 12 - 14, 2016, pp. 1-4.

[21] Yang, M.-J., Jhou, H.-L., Ma, B.-Y., and Shyu, K.-K., "A Cost-Effective Method of Electric Brake With Energy Regeneration for Electric Vehicles," IEEE Transactions on Industrial Electronics, vol. 56, issue 6, pp., 2203 – 2212, June 2009.

[22] A. Mohammad, M. A. Abedin, and M. Z. R. Khan, "Microcontroller Based Control System for Electric Vehicle," International Conference on Informatics, Electronics & Vision (ICIEV 2016), pp. 1-4, May 2016.

[23] Mohammad, A.; Ziaur Rahman Khan, M., "BLDC motor controller for Regenerative Braking," in Electrical Engineering and Information Communication Technology (ICEEICT), 2015 International Conference on , vol., no., pp.1-6, 21-23 May 2015.

[24] Bo Long, Shin Teak Lim, Ji Hyoung Ryu and Kil To Chong, "EnergyRegenerative Braking Control of Electric Vehicles Using Three-Phase Brushless Direct-Current Motors," Energies, vol. 7, pp. 99-114, January 2014.

[25] M.K Yoong, Y.H. Gan, O.D. Oan, C.K. Leong, Z.Y. Phuan, B. K. Cheah and K.W. Chew, "Studies of regenerative braking in electric vehicle," in 2010 IEEE Conference onSustainable Utilization and Development in Engineering and Technology (STUDENT), Nov. 2010, pp. 40-45.

[26] R. F. Coughlin, F. F. Driscoll, "Introduction to Op Amps," in Operational Amplifier and Linear Integrated Circuits, 6th ed., New Delhi, India: Prentice Hall of India Private Limited, 2009, pp.1-12.

[27] M. H. Rashid, "Diode Rectifiers," in Power Electronics Circuits, Devices and Applications, 3rd ed. New Delhi, India: Prentice Hall, 2014. pp. 68-121.

[28] “ Arduino & Genuino Products > Arduino/Genuino UNO, ” January 2013. [Online]. Available: https://www.arduino.cc/en/Main/ArduinoBoardUno. [Accessed: January 2015].

[29] “A Beginner’s Guide to the MOSFET,” September 2011. [Online]. Available: https://reibot.org/2011/09/06/a-beginners-guide-to-the-mosfet/. [Accessed: Jan. 21, 2016]

[30] “BLDC Motor Control With Arduino, Salvaged HD Motor, and Hall Sensors,” 2016. [Online]. Available: http://www.instructables.com/id/BLDC-Motor-Control-with-Arduino-salvaged-HD-motor/step6/Hall-Sensor-Circuits/. [Accessed: Feb. 05, 2016].

[31] “Consider New Designs When Selecting Hall Effect Sensors for BLDCs,” March 2014. [Online]. Available: http://www.e-driveonline.com/main/articles/consider-new-designs-when-selecting-hall-effect-sensors-for-bldcs/ . [Accessed: Mar. 07, 2016].